POLITECNICO DI TORINO

Master Course in Aerospace Engineering

Master Thesis

Design and Development of a Test Bench for Frequency Analysis of FBGs Optic Sensors for Prognostic Techniques for Aerospace Applications

Supervisor:
Prof. Paolo Maggiore
Co-supervisor:
Ing. Matteo D.L. Dalla Vedova

Candidate:
Gioele Baima

March 2019

Acknowledgement

I would sincerely like to thank my supervisors, the whole PHOTONEXT team and all the people who helped me and with this thesis work. In particular I would like to thank the professor Paolo Maggiore, Ing. Matteo D.L. Dalla Vedova and Dott. Piercarlo Berri for their fundamental advices, suggestions and especially for the time that they dedicated to me, moreover a special thanks goes to Dott. Matteo Facciano who helped me both with the optic aspect of the work and during the writing of the thesis. I would like to thank my colleagues: Giuseppe, who worked with me for the whole duration of the project, Bruno, Denny, Guido, Rachele and Alice with whom i shared my time, we sustained each other and enjoyed ourself together. I would like to thank all of my friends who supported, helped and spend their time with me in all of these years.
A fundamental thanks goes to my parents and my family, that with their sacrifices permitted me to complete this formative path, and to my girlfriend Margherita, who has always sustained me in these years.

Abstract

The purpose of this thesis is studying the frequency response of the FBGs optic sensors, obtaining in this way their characterization, informations of fundamental importance in order to develope a future vibrations sensor using the fiber optic.
It will be shown how the test bench has been designed and developed, in order to conduct a dynamic analysis of the fiber. The bench setup has been strongly influenced by the previous PHOTONEXT research works, making them solidal with this new aspect of the research, but it has been modified to match with the new hardware devices needs. Regarding the hardware compartment two blocks are presents: the device which reads the optic sensors measurements and the device which acts as a vibration source.
The fiber dynamic behaviour will be hence analyzed comparing the measures obtained by the laser interrogator with the signal provided by the vibrations source. Since that each device has its own software, which provides its measures, a new code has been written to put them in communication.
Besides the measures results, all the factors which can affect them, such as the amplitude of the signal or the repetability of the tests, will be taken into account.
As conclusions, all the limits relative the designed test bench will be exposed and some advices and tips will be given, with the aim of improve the code potentiality and develope a new test bench, which will actually be a vibration sensor.

Contents

List of Figures

List of Tables

Introduction

This thesis is one of the projects of the PHOTONEXT research group, carried on by professors and students of the DIMEAS, Mechanical and Aerospace Departments, of the Politecnico di Torino, and with the contribute of the ISMB, Istituto Superiore Mario Boella.
The PHOTONEXT group works focus on the use of the fiber optic as a sensor in many aerospace applications: it is trying to validate the Fiber Bragg Grating sensors in place of the traditional sensors.
The previous works of the research group focused on temperature relevaments and static measurements, this thesis work lays the foundation for a complete dynamic analysis of the optic sensors.
The use of the optic fiber as a sensor is a significative improvement in sensing applications: it is really light, it doesn't need to be powered, it can transmits a great amount of data and it is immune to electromagnetic field, howewer, to read the data a laser interrogator is necessary. A complete review and a detailed description of the fiber optic and the Fiber Bragg Gratings are given in chapter 1 and 2.
In order to conduct a dynamic analisis the motion must be provided to the fiber. Different solutions can be used, for example a speaker or a frequncy generator, in this thesis a piezoelectric actuator has been chosen. The actuator system has presented both advantages and disadvantages: the main advantage is the presence of its software, by means of which is possible to command it without using code lenguages, but it also have disadvantages, as the system attenuation and the frequency range limitations. A detailed description of its features, how it works, how to command it and the controller logic are explained in chapter 3 and 5.
A detailed description of each component of the test bench developed is in chapter 4, while chapter 5 describe the interrogator and the piezoelectric ac-

tuator softwares. Chapter 5 also explane the code written to put in communication and analyze the values of these two instruments, and the MATLAB script which provide the tests results as an amplitude Bode diagram.
Once listed the features of hardware, software and the written codes, the thesis will provide the tests results and some observations regarding the fiber behaviour, it will examine the influence of several factors on the test results and it will explane the physical reasons at the base of the obtained results.
The Future works section gives useful informations on the base of the experience matured by working with these devices and the relative softwares , in particular it provides precise advices and tips on which basing the new code and the new test bench development.

Chapter 1

Optical Fibers

Optical Fibers are filaments, usually made of glass or polymeric materials, which carry the light to long distance with a minimum signal attenuation, exploiting the total reflection principle.
Historically used in the telecommunication sector as data transportation system, optical fibres are nowadays also used as sensors. This, combined with the excellent physical characteristics (very small weight and size) promotes their diffusion in new engineering sectors such as, for example, aerospace.
A general description, the working principle and the main advantages of the fibres will be explained in the next sections.

1.1 Materials

A first classification considering the materials which compose the optical fibers can be made. These, in fact, affect several properties of the fibers: for example reflectivity, changing the attenuation value, or mechanical properties, i.e. robustness. It is therefore necessary to select the proper material which better suits the task required; the most common are glass and plastic (or polymer).
Glass optical fibers are made from ultra pure-silica which permits a low attenuation value, ≈ 0.2 dB/km [1], and good optical properties over a wide range of wavelength, these characteristics make this type of fibers perfect to a long range applications.
Moreover silica can be doped, usually with germanium or boron, in order to

raise or lower the refractive index.
They also have some disadvantages: they are brittle, a small radius of curvature breaks the fibers, and they are more expensive than the polymerics ones.
Polymeric (or plastic) optical fibers (POF) have been developed as a cheaper alternative to traditional fibers, they have improved mechanical properties (greater strength and flexibility), but a worse attenuation value than traditional ones [2].
Attenuation value is $\approx$ 0.1 to 1 dB/m making this fibers perfect for short-range application [3].

1.2 General Description and Classification

An optical fiber, as shown in figure 1.1, is made up of several concentric layers that differ in diameter and thickness.

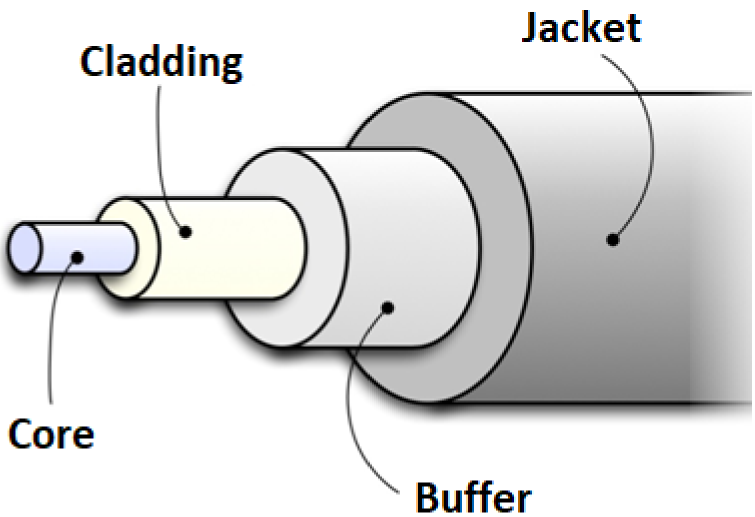

Figure 1.1: Generic composition of an optical fiber

The core is the inner layer, made of a dielectric material, through which the light is reflected; the core is surrounded by the cladding layer which has a different refractive index that keeps the signal confined within the core. The

latter has usually a diameter of $\approx 125\ \mu m$ [1].
The buffer wraps the cladding, providing the resistance to mechanical stresses and protecting the fiber from humidity, which can affect the performance; buffer diameter is $\approx 250\ \mu m$. The outer layer is named *Jacket*, it works as a shield for the internal layers, dividing the whole fiber from the outside environment, its diameter is $\approx 400\ \mu m$.
The core layer varies in dimensions from 8 μm to 50 μm or 62.5 μm [1], depending on the way the light is transmitted. It is then necessary to provide a first classification of the fibres considering light's propagation modes [2] :

- $single-mode\ fibers$, named also mono-mode, supports only one mode of light transmission;
- $multi-mode\ fibres$, supports more than one way of light transmission.

Bigger core dimensions increase the value of the fiber's numerical aperture[1], permitting to carry a greater amount of light and gather it more easily, so that cheaper electronic sources as LED can be used.
Different types of dispersion, for example modal dispersion[2], affect multi-mode fibers, increasing signal losses and making them ideal for short haul applications (100-2000 m at 10 $Gbit/s$-100 $Mbit/s$) [2]. Single-mode fiber are instead ideal for long haul transfer, thousands of km with low data losses and bitrate over 10 $Gbit/s$.
Another type of classification is the inner layers refraction index profile [2] (core and cladding) :

- $step\ index\ profile$, for single-mode and multi-mode fibers;
- $graded\ index\ profile$, only for multi-mode fibers.

The core index of refraction, n_1, and the cladding, n_2, of a step index profile are uniform and constant along the layer; the transition from the value n_1 to the value n_2 occurs suddenly, this implies that every ray of light reaches the end of the fiber at different time causing modal dispersion.
To avoid modal dispersion, multi-mode graded index fibers have been developed, the value of the refractive index of the core decreases according to the

[1]See 1.5

[2]It is a distortion mechanism of the optic signal due to different speed of the modes of the light [3]

distance from the center, while the value of the cladding is constant.

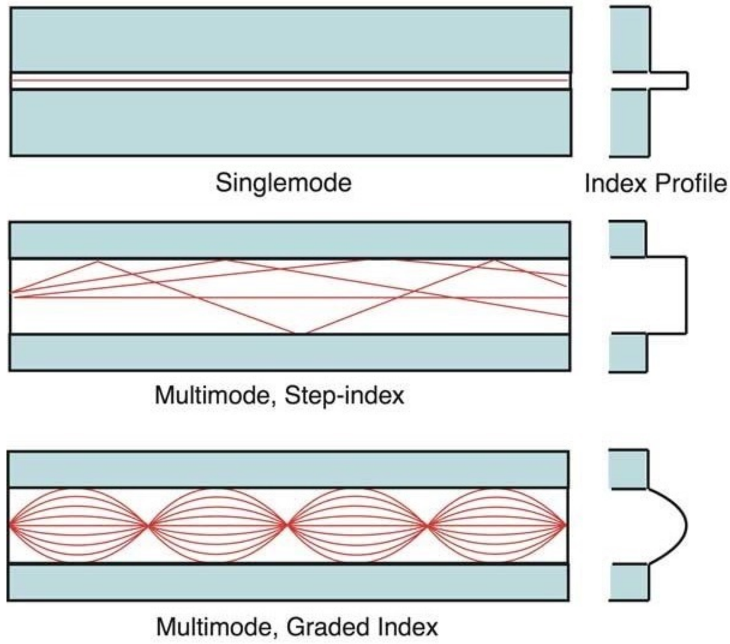

Figure 1.2: Difference between step and graded index

As visible in figure 1.2, the light rays in the graded index follow a sinusoidal, nearly parabolic, path due to the variation of the core refractive index, forcing the different rays to reach the same position in the same time [3].

1.3 Working Principle

Optical fibers working principle is based on the mechanism of the light refraction described by the *Snell's law*, in particular the total reflection phenomenon.
To understand the total internal reflection (or TIR) it is first necessary to define the refraction index n as :

$$n = \frac{c}{v} \tag{1.1}$$

where:

- n is the refractive index of the medium, this number quantifies how much the propagation of light is faster in the vacuum than within a material;
- c is the speed of light in vacuum;
- v is the speed of light in medium

Considering a glass made optical fiber, a typical value of refractive index of the core is $\approx$ 1,5 (n_1), while typical value of cladding refraction (n_2) is $\approx$ 1.475, however values change depending on the doping element.
It is possible now to introduce the *Snell's law*:

$$n_1 \cdot sin\theta_i = n_2 \cdot sin\theta_t \tag{1.2}$$

Where :

- n_1, n_2 are the refractive indices of the medium;
- θ_i is the incident angle of the light ray;
- θ_t is the angle of the refracted ray.

The angle θ_t, supposing n_1 and n_2 constant, vary only depending on the incident angle, as shown in figure 1.3.

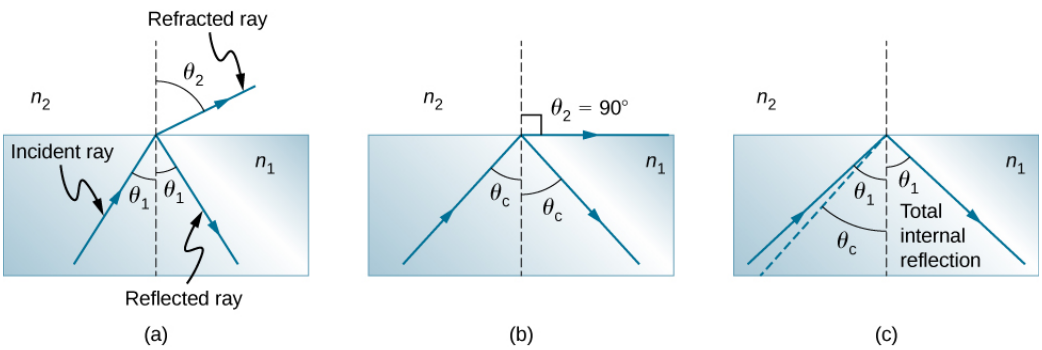

Figure 1.3: Variation of the refracting angle considering $n_2 < n_1$.
(a) generic situation; (b) critical situation; (c) total reflection phenomenon

It is then possible to define the critical angle, the incident angle θ_c for which the refracted angle $\theta_t = 90°$, for all the angles $\theta_i > \theta_c$ total internal reflection occurs.

$$\theta_c = arcsin\left(\frac{n_2}{n_1}\right) \cdot sin\left(\frac{\pi}{2}\right) = arcsin\left(\frac{n_1}{n_2}\right) \tag{1.3}$$

Figure 1.3 shows the behavior of a ray that is already inside the fiber, it is also necessary to describe with which angle the ray of light has to affect the core so that TIR occurs. This angle is named *acceptable angle*, α_{max}, and it is obtainable in a few steps according to figure 1.4

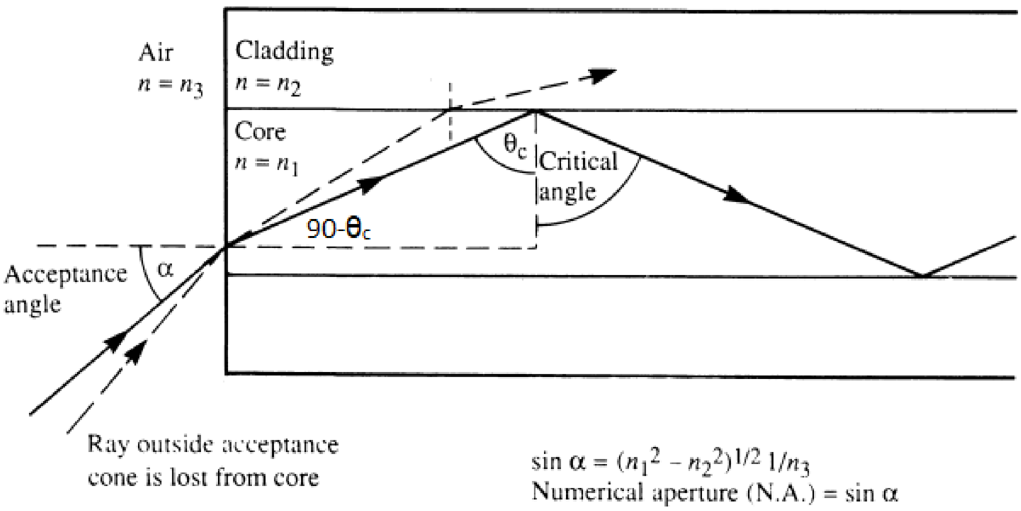

Figure 1.4: Acceptable angle of an optical fiber

Applying Snell's law between air, n_3, and core, n_1:

$$n_3 \cdot sin\alpha_{max} = n_1 \cdot sin(\frac{\pi}{2} - \theta_c) \tag{1.4}$$

Considering $sin(\frac{\pi}{2} - \theta_c) = cos\theta_c$ and squaring both sides:

$$\left(\frac{n_3}{n_1}\right)^2 \cdot sin^2\alpha_{max} = cos^2\theta_c = (1 - sin^2\theta_c)$$

Reminding the equation 1.3 and expliciting $sin\theta_c = \frac{n_2}{n_1}$:

$$\left(\frac{n_3}{n_1}\right)^2 \cdot sin^2\alpha_{max} = 1 - \left(\frac{n_2}{n_1}\right)^2$$

So:

$$sin\alpha_{max} = \frac{\sqrt{n_1^2 - n_2^2}}{n_3} \tag{1.5}$$

The numerator of the equation 1.5 is called *numerical aperture*.

$$NA = \sqrt{n_1^2 - n_2^2} \tag{1.6}$$

1.4 Advantages and Disadvatanges

The use of optical fibers in data transfer has many advantages if compared to the traditional copper transmission:

- the main advantage of this technology is the large amount of data, which is able to be transferred at high speeds. Also, the low signal attenuation allows data to be sent over long distances [2];
- fibers are much more light weighted than copper, allowing them to transfer the same quantity of data with a significantly reduced weight. Optical cables are also smaller and more flexible making them easier to install [2];
- fibers have no interaction with electromagnetic fields. Their performance can't be affected by space cosmic radiations or electronical devices' electromagnetic fields, making them perfect for aerospace application [2].
- glass is more abundant then copper, making the fibers cheaper to realize.
- glass is an insulating material so it doesn't carry current. This eliminates the possibility of spark and fire hazards [2].

Some disadvantages of the fibres:

- they can't be installed with small curve radius, these can break the fibers or affect their performance increasing the losses [2];
- installation and equipments needed to use the fibers as sensors are expensive;
- splicing[3] requires high precision and expensive instrument. A good splicing quality is needed to avoid losses.

[3] Joining two fibers or a connector to a fiber

Chapter 2

Optical sensors: Fiber Bragg Gratings

The optical fiber, in addition to its traditional use (data transmission), is finding a new application in the sensoristic field; it is possible to measure several physic quantities: for example temperature, strain, pressure, stress, vibration and many others.
The *optical fiber sensors* (or OFS), unlike the traditional sensors, work passively, so no electrical alimentation is needed, representing the main advantage of this technology.
Sensors have other advantages:

- they are an integral part of the fiber, this means very small sizes and weight [4];
- thanks to fiber characteristics they are immune to electromagnetic fields [4];
- they have signal's multiplex ability[1] [1]. This, in addition to their development, is making them cheaper.

The main disadvantage is the high cost of the instrument necessary to read sensors values.
A large number of sensors have been developed, fibers used in this thesis are equipped with *Fiber Brag Gratings*, or FBG.

[1]It is possible to use a single instrument to control several sensors

2.1 Fiber Bragg Grating Classification

A Bragg sensor is a diffractive grating made by means a periodic variation of the core's refractive index.
When a light ray passes through the Bragg structure, it gets reflected at each refractive index variation. The combination of all these reflected light components produces a large reflection at a determinate wavelength, denominated Bragg wavelength λ_B [4] [18].
An analytical analysis is given in section 2.3.
Figure 2.1 shows a FBG's uniform structure, $n3$ is the core's refractive index variation.

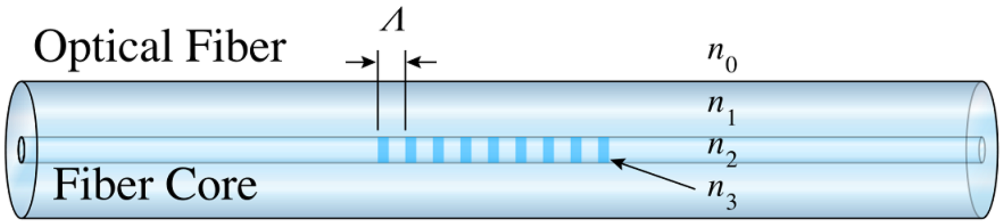

Figure 2.1: Structure of a Bragg grating

Sensors are divided into two main categories: *short period Bragg gratings* and *long period Bragg gratings*. The difference from short to long period is, precisely, the grating period Λ, in short period ones Λ is $\approx$ hundreds of nm, in long period ones Λ is fraction of millimeters [5]. In this thesis *short period Bragg gratings* are used.
Several short period structures have been developed in the years, modifying the way and the direction in which the refractive index varies or modifying the grating period [5] [6]:

- $uniform\ gratings'$ refractive index follows an armonic variation. Uniform FBGs are used in this thesis and their working principle will be explained in section 2.3; UFBGs structure is shown in figure 2.1.

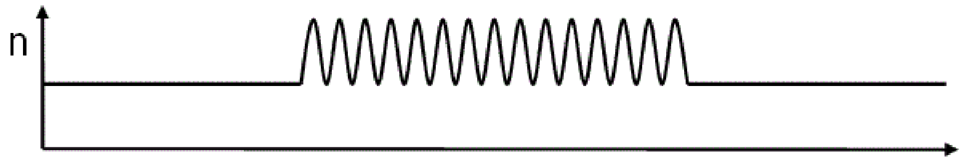

Figure 2.2: Refractive index variation of uniform grating

- *apodized gratings* use refractive index variatons to control the side lobes[2] strength, suppressing them and maintaining other properties as reflectivity and narrow bandwith. Two main shape of the refractive index are used: the Gaussian one, figure 2.3 (a), and the cosine one, figure 2.3 (b);

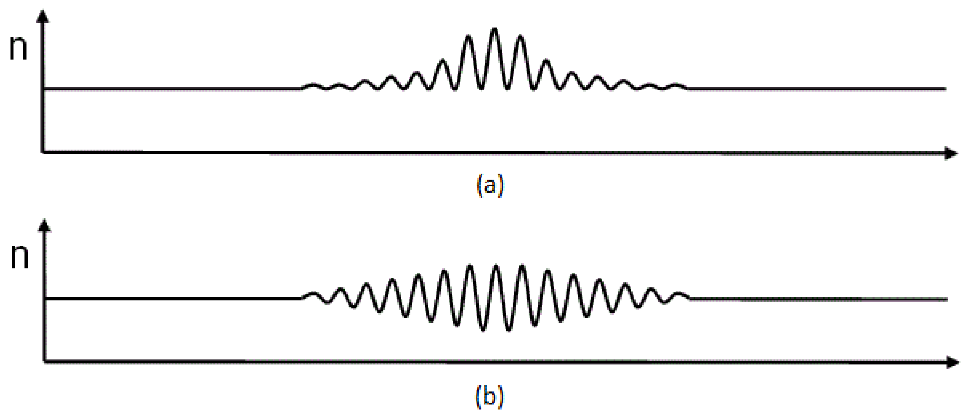

Figure 2.3: Refractive index variation of apodized grating, Gaussian(a) , cosine(b)

- *phase shifted gratings* are sensors in which a π phase shift is addicted to the refrative index, usually in the center of the grating, in order to modify its reflective spectrum.

[2]Side lobes are regions of the transmitting area of an antenna which aren't the main lob

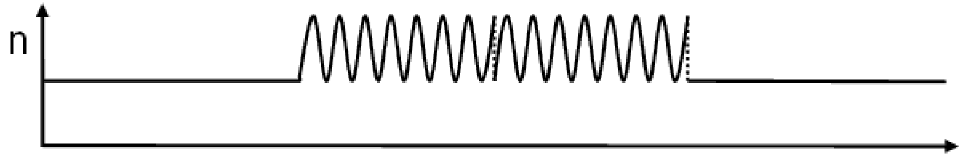

Figure 2.4: Phase shifted Bragg structure

- *chirped gratings* are sensors in which the grating period Λ is varied, a typical Λ variation is the linear one. LCFBGs have a very high resolution and they are used to control some type of dispersions, i.e scattering; their structure is visible in figure 2.5.

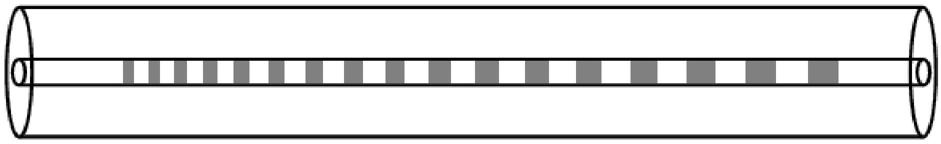

Figure 2.5: Chirped Bragg structure

- *tilted gratings* have, like uniform ones, constant Λ value; the difference from UFBGs lies in the modulation of the refractive index. As visible in figure 2.6 n modulation isn't normal to the axis fiber but it is tilted of an angle θ, which usually varies from $2°$ to $20°$. Tilt angle θ is set during manufacturing processes and it controls the spectral profile of the grating.

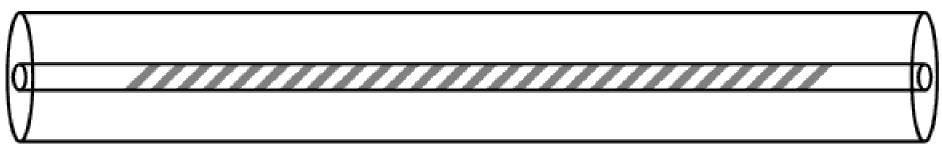

Figure 2.6: Tilted Bragg structure

2.2 FBG manufacture

FBG sensors are written inside the core with intense ultraviolet sources such as UV laser; intensity and exposure of the fiber to UV source determine the characteristics of the grating, and so the wavelength reflected.
The property which allows the inscription of the sensor inside the fiber is the *photesensivity*.
Photosensivity is a permanent variation of optical fiber's refraction index when exposed to high intensity light sources of certain wavelength, usually UV. UV rays, which can be pulsed or continuous, damage at atomic level the optical fiber, changing permanently its n value. Pure silica fibers are not suitable for this technique so they are doped with high level of Germanium, in order to achieve better photosensive characteristics. Same results can be reached with hydrogenation, a process in which fibers are soaked in a high pressure hydrogen chamber at temperature from 20° to 75°, in order to increase the hydrogen concentration within the silica fibers [1].
Several method have been developed, in the following pages the main ones will be explained: *Photomasking*, *Interfering Beams* and *Point by Point*.

2.2.1 Phasemasking

A thin silica diffractive mask is placed between the fiber and the light source, when exposed to UV rays it diffracts in ± 1 direction, suppressing 0 order diffraction (perpendicular to fiber axis), as visible in figure 2.7. Mask surface has periodic grating corrugations with period Λ_{pm}, which produce an interference fringe on the fiber with periodicity $\Lambda = \frac{\Lambda_{pm}}{2}$. Moving along the fiber axis the UV source is possible to create long Bragg sensors, it is also possible to manufacture chirped FBGs, chirping the phase mask, and tilted ones, tilting the mask of the value of θ [1].
This process has the lowest cost per Bragg grating and a good repeatability but it is necessary to remove the jacket from the optical fiber, weakening its structure and tensile strength. In addition to this each mask has its wavelength, so different masks are neeeded for each Bragg wavelength [1].

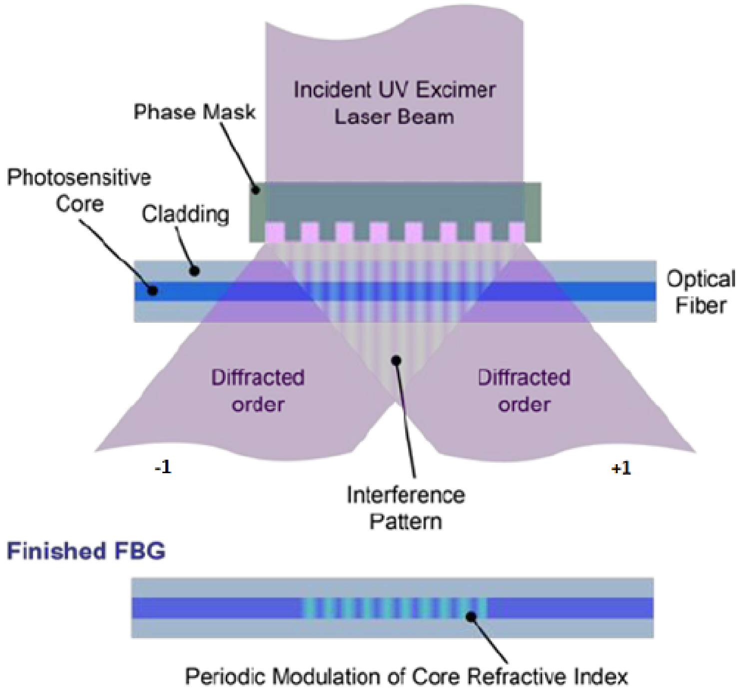

Figure 2.7: Phasemasking method

2.2.2 Interfering Beams

UV rays, once emitted by the source, are then divided into two beams by means of a splitter, these propagate in the air until they reach an orientable mirror. Mirrors reflect rays with an angle θ and then are focused, passing through cylindrical lens, on the fiber, where FBG is inscripted.
This process is strongly affected in performance by the tolerance of each component, such as the mirror, and it is necessary a perfect set up to achieve good results, in fact both beams must be perfectly focused with a certain angle on the fiber's core.
Considering this it is clear that a software support is essential to control mirror orientation and activation of the UV source.
With this method is virtually possible to create Bragg grating of every Λ value and wavelenght, it is possible to fabricate CFBGs and TFBGs. Like photomasking process, fiber's jacket has to be removed [1].

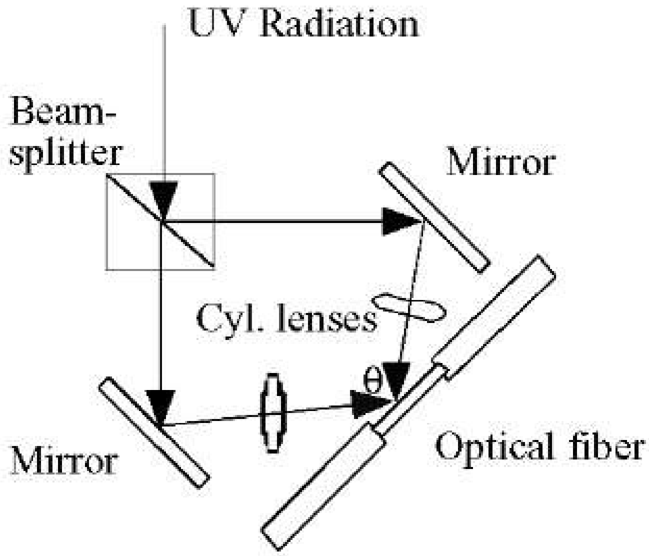

Figure 2.8: Interfering beams generic scheme

2.2.3 Point by Point

This technique focuses high energy impulses directly within the fiber core with high precision. Fiber is moved each time of the Λ quantity desired, until the end of the grating is reached.
The main advantage of this method is the possibility to create the sensor without removing the fiber's jacket [1].
On the other hand the process has some significant disadvantages: it is a slow process; it requires a precise fiber movement control system; the grating produced exhibit strong sidelobs which heavily affect the wavelength estimation.

2.3 Working Principle of the FBG

FBG works as a filter, it allows some frequencies to pass and reflects others. In figure 2.9 is shown the working principle of a fiber Bragg sensor.

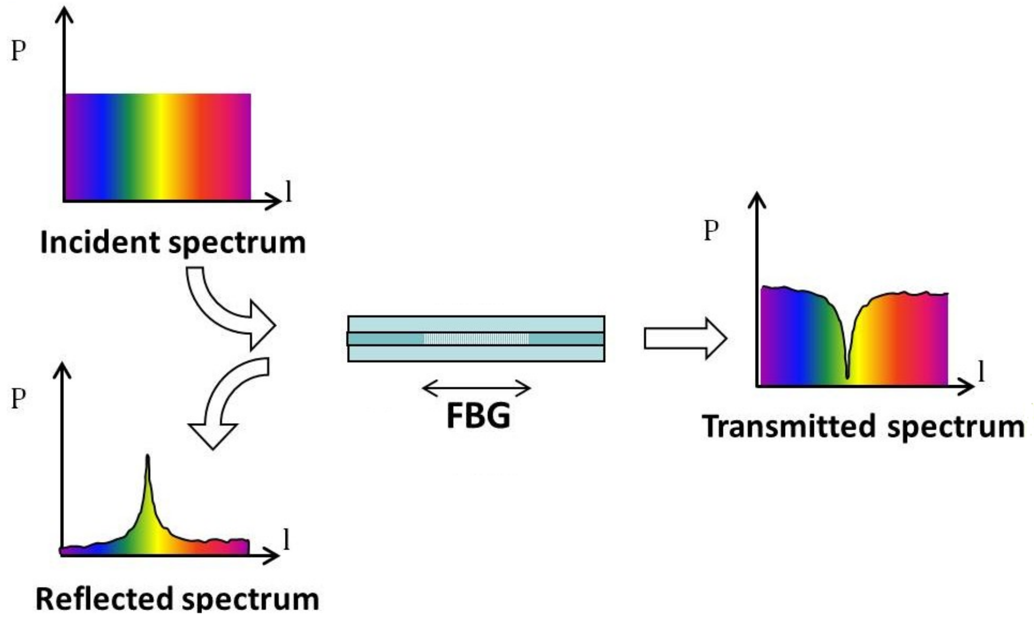

Figure 2.9: Bragg sensor working principle

Fundamental equation of Bragg grating is:

$$\lambda_B = 2 \cdot n_{eff} \cdot \Lambda \tag{2.1}$$

where:

- λ_B, Bragg reflected wavelength;
- n_{eff}, effective refractive index of the grating's core;
- Λ, grating period.

Strain and temperature affect Bragg's reflected wavelength, according to [7]:

$$\Delta\lambda_b = \Delta\lambda_S + \Delta\lambda_T \tag{2.2}$$

$\Delta\lambda_b$ is the variation of reflected wavelength due to $\Delta\lambda_S$, strain induced wavelength shift, and $\Delta\lambda_T$, temperature induced wavelength shift.
Exploiting the terms $\Delta\lambda_T$:

$$\Delta\lambda_T = \lambda_B(\alpha + \xi)\Delta T$$

and $\Delta\lambda_S$ as:

$$\Delta\lambda_S = \lambda_B(1 - P_e)\Delta\epsilon$$

It is possible to write [7]:

$$\Delta\lambda_b = \lambda_B(1 - P_e)\Delta\epsilon + \lambda_B(\alpha + \xi)\Delta T \tag{2.3}$$

where:

- P_e, Photoelasticity constant;
- $\Delta\epsilon$, strain;
- α, thermal expansion coefficient;
- ξ, thermo-optic coefficient;
- ΔT, temperature variation.

In figure 2.10 is shown the effect of strain on a FBG, as visible grating period Λ is increased, this produces a shift of the Bragg reflected wavelength.

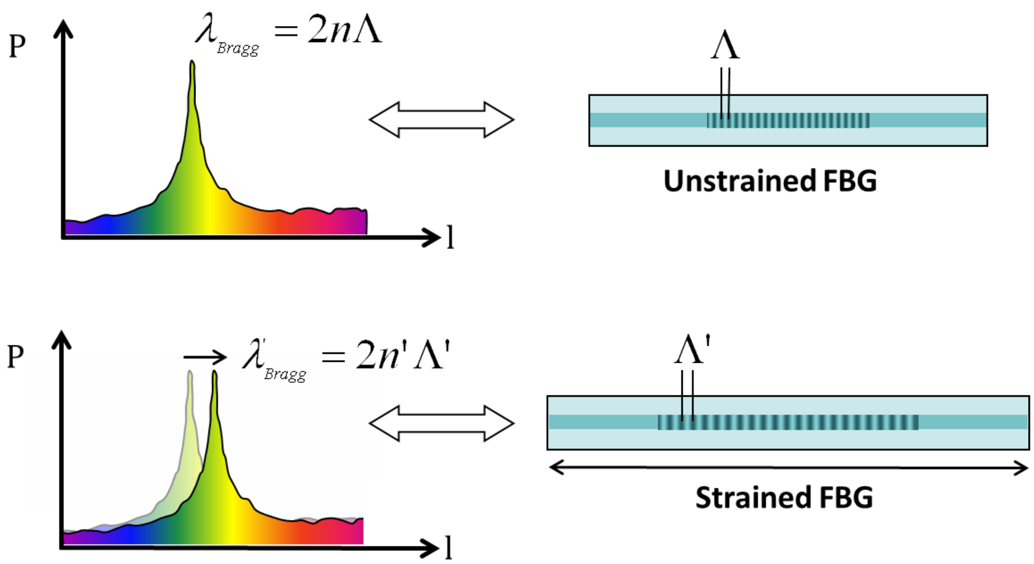

Figure 2.10: Strain effect on a FBG

Chapter 3

Instruments Features

Two sets of instrument are necessary to realize a dynamic analysis of the fiber: one has the task to provide the motion to the fiber while the other one reads the deformation to which the Bragg grating is subjected.
The motion is provided by a *Piezoelectric* device, controlled in current and tension by its power supply.
The measurements are taken by a laser interrogator, which has already been used in previous research works, like static and thermal characterization of the fiber.

3.1 Laser Interrogator Set

An interrogator is a device that can acquire information about the optical fiber behaviours by sending laser beams to the Bragg grating, evaluating its response. The data acquired can refer to different physical quantities, depending on the interrogator used: it can provide information on wavelength, strain, temperature or pressure, to which the fibers , and so the Bragg sensors, are subjected.
The interrogator used in this thesis is the *Smartscan SBI* model.
Here are the interrogator's main features [8] :

- **Number of optic channels**: 4, four different fibers can be interrogated at the same time;

- **Max sensors per channel**: 16;

- **Interrogation range**: 40 *nm*, only fibers with wavelength from 1528 to 1568 *nm* can be interrogated;
- **Max Scan frequency with all sensors simultaneously**: 2 500 Hz;
- **Max Scan frequency single sensor**: 25 000 Hz;

Figure 3.1 shows the *Smartscan SBI*, as visible it is an electronic module without any type of coverage.

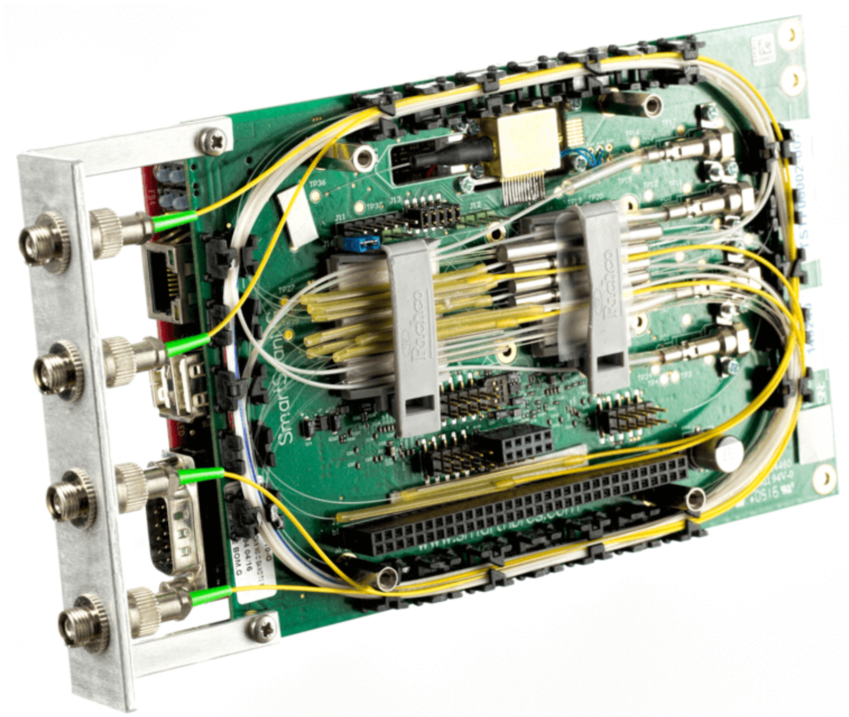

Figure 3.1: Smartscan SBI module [8]

To avoid cortocircuits, dust deposition and other type of accidental damages, the module has been installed into an artigianal coverage.
The interrogator works only if connected to its software, *Smartscan 4.1.1*, which has to be installed on the computer; the connection can be done in different ways: via USB, via Ethernet cable or via RS-232. The fastest one is the Ethernet port, so it is recommended its use to process and save the measurements' data.

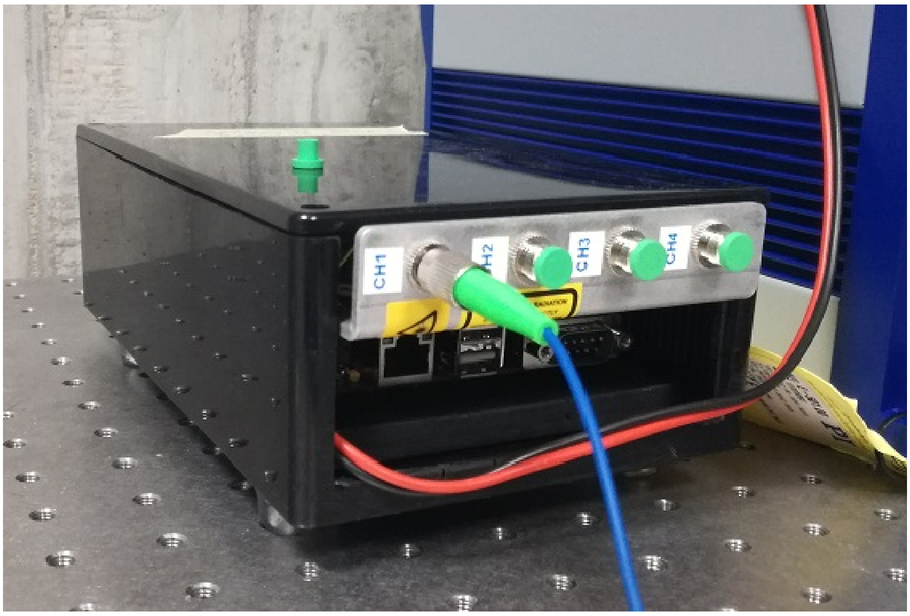

Figure 3.2: Smartscan SBI coverage

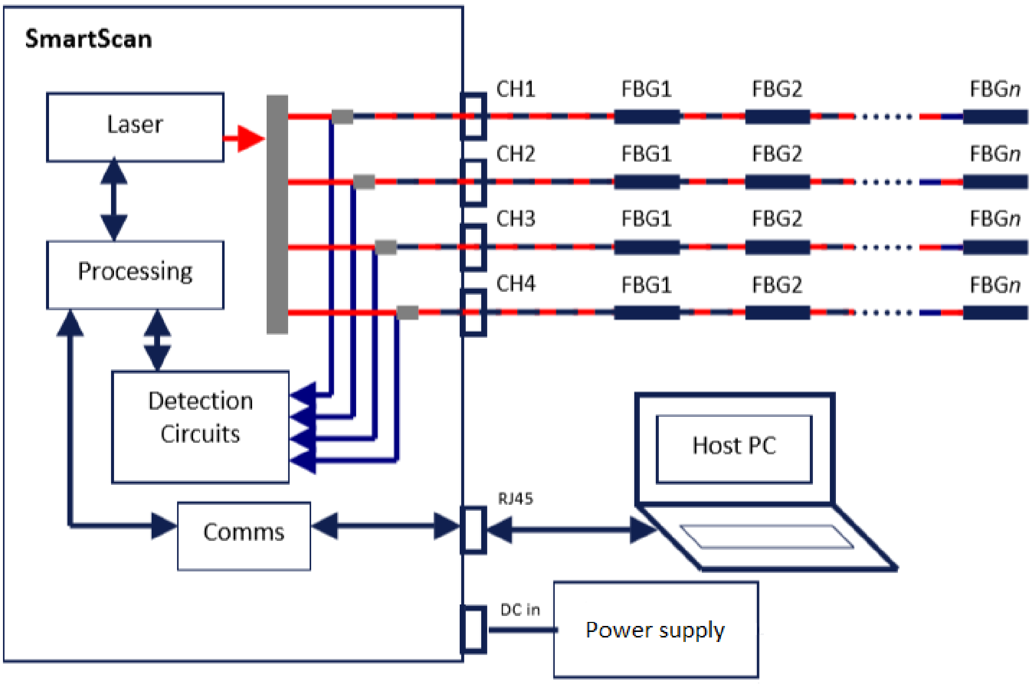

Figure 3.3: Interrogator set layout and flux diagram

The interrogator instrument set is then composed by a host pc, where the control software is installed, and the interrogator itself, to which fibers (equipped with Bragg sensors) are connected. Figure 3.3 shows the layout and provides a basic flux diagram of the SBI module.
The software is the interface on which is possible to customize, start and save the measurement, a more detailed explanation will be given in chapter 5.

3.2 Piezoelectric Set

The term *Piezoelectric set* refers to all the tools necessary to provide the movement to the fiber. The piezoelectric set used in this thesis has been bought from the *Physik Instrumente (PI)* company.
The set is composed by:

- a piezoelectric actuator;
- a modular piezo controller;
- an interface software.

Before providing a description of the instruments used to make the measurement, it is necessary to understand what is a piezoelectric material and how it works.

3.2.1 Piezoelectric Phenomenon

Piezoelectric materials are part of the category denominated *Smart materials*, the term "smart" refers to the materials' ability to quickly respond to certain external stimuli, producing a variation of their physical properties. External stimuli are numerous and of different nature, example are pressure, temperature, mechanical deformation, electric fields, nuclear radiations and many others. These produce, for example, a variation in shape, colour, damping or generation of electric dipoles within the materials [9].
The *piezoelectric phenomenon* was discovered in 1880 by the Curie brothers, they found that non-centrosymmetric crystals, such as quartz, produce electric dipole (and so electric charge) if subjected to compression, or more in general to mechanical deformations.

A year later, Gabriel Lippman discover the *converse piezoelectric effect*, according to which these materials have a geometric deformation proportional to the applied electric field [9].
During the years following the discovered of the phenomenon, in particular in the world wars ages, several piezoelectric materials were found. Experience and work method matured in these years led to two big family of piezoelectric materials: piezoceramics, the most used, and piezopolymers [10].
The most common piezoceramic material is the PZT, or lead zircon titanate. It is an inorganic compound developed in 1952 at Tokyo Institute of Technology and made by lead, zirconium, titan and oxygen; its structure is represented in figure 3.4.

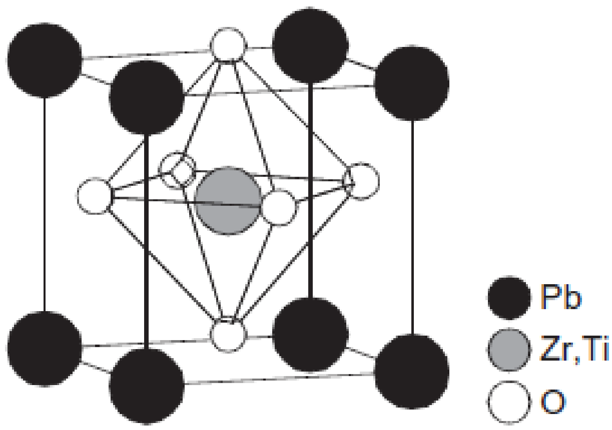

Figure 3.4: PZT internal structure [10]

The piezoelectric materials can be used in the sensors field, in particular they find application in accelerometers, strain sensors, pressure transducers, actuators and vibration sensors [10].

3.2.2 Piezoelectric Actuator

The actuator used in this thesis is the *PI P753.31C*, made of PZT.
The converse piezoelectric phenomenon is exploited to make the actuator move, according to the applied tension from the controller to which is connected by 3 wires.

It is possible, by means of threaded holes, to fix external supports, such as plates or masses, to two different surfaces of the piezo device. As visible in figure 3.5, six holes have been obtained on the top face of it while the side face owns only two. In the configuration shown in figure 3.5, the motion will be provided along the horizontal axis, however, it is also possible to move the actuator in vertical direction by rotating it.[1].

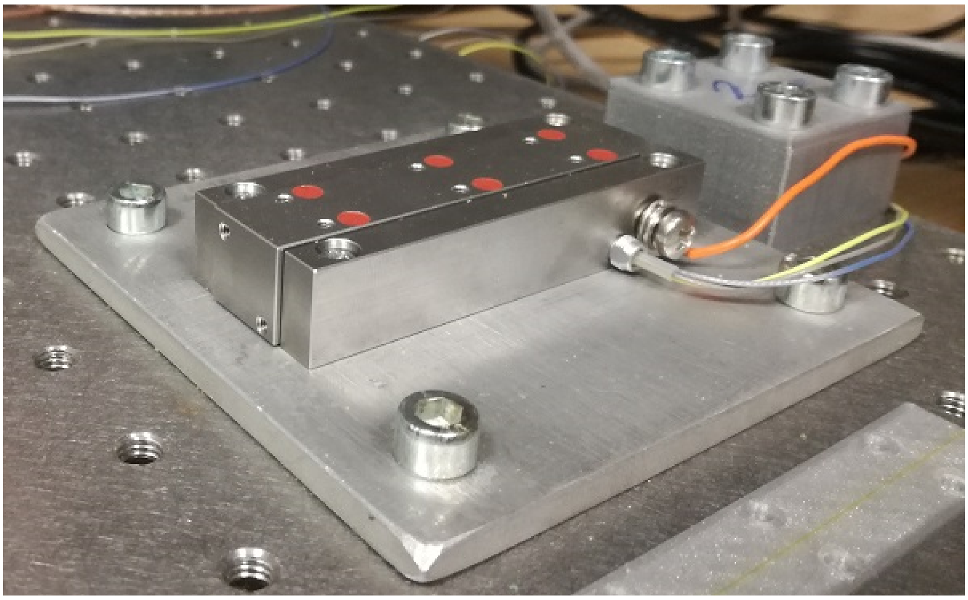

Figure 3.5: *PI P753.31C* Piezoelectric actuator

The masses and the external supports have to be centered when mounted on the piezo's surface: a wrong mass distribution above it may cause undesired oscillations or resonance phenomena which can permanently damage the actuator, especially at high frequency (from 500 to 1000 Hz).
Upper and side faces have different mass load limits: according to figure 3.5 configuration, the top face allows a maximum mass load of 2 Kg while the side face's maximum load is 10 Kg.
In table 3.1 are shown the piezoelctric actuator's main features, complete informations are available on *PI piezoelectric datasheet* [11].

[1]obviusly once the piezo is rotated, the side face considered in the setup of figure 3.5 setup will become the vertical face.

Dimensions [mm]	80 x 30 x 15
Mass [Kg]	0.26
Load capacity [Kg]	2/10
Resolution [nm]	$\pm$ 3
Travel range [μm]	0 - 38
Natural frequency [KHz]	2.9
Max operating frequency [KHz]	1.0
Max operating voltage [V]	-20 to 120

Table 3.1: *PI P753.31c*'s main features

3.2.3 Piezo Controller Module

Physik Instrumente also realized the piezo's controller unit, this is in turn composed by several submodules, which are substantially electronic boards, installed within a protective case.

Figure 3.6: *PI* Piezo controller module

The piezo controller module, shown in figure 3.6, has the task to provide the correct power supply to the actuator, in order to make it move as commanded.

The instrument is then composed by:

- *E-501* chassis, within the electronic boards are installed;
- *E-518*, is the interface module;
- *E-509.C1A*, is the sensor and controller module;
- *E-504.00F*, is the amplifier module.

Figure 3.7 shows signal's path and the modules interconnection.

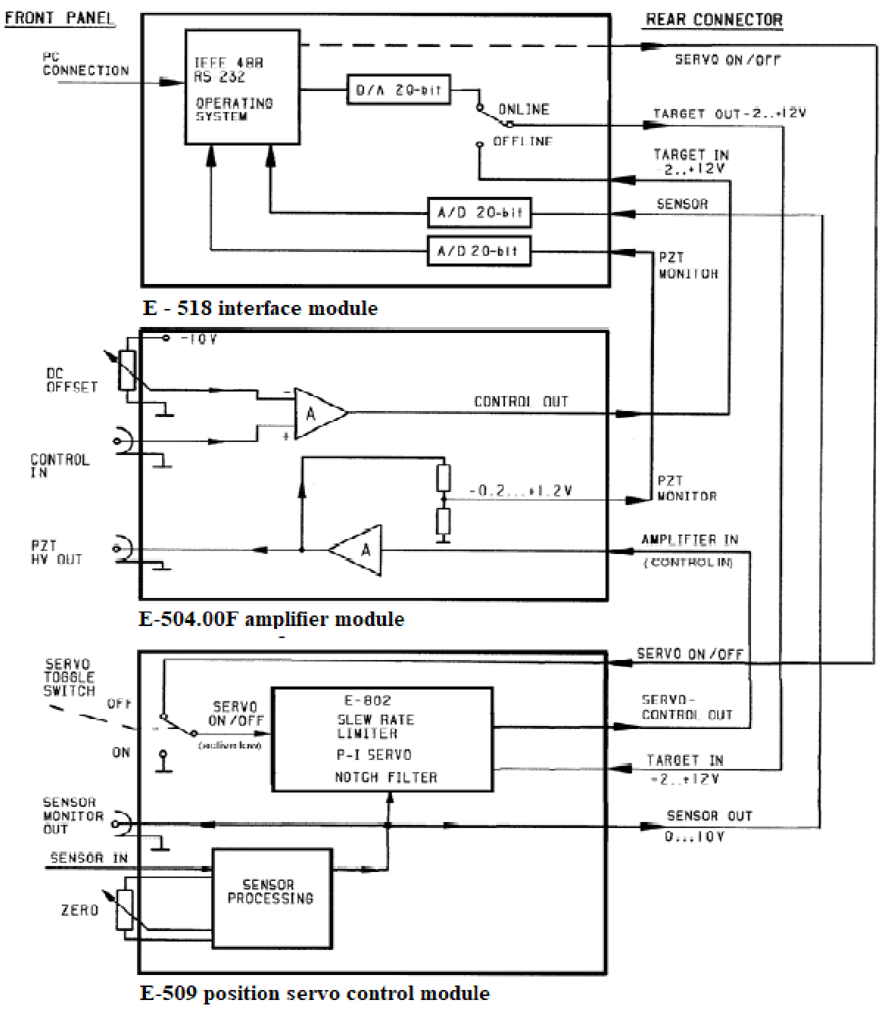

Figure 3.7: Signal logic [13]

The piezo controller unit can be commanded in analog way, providing directly the tension, or digitally, using a software to set the input by means of a computer. Let's take a look, from figure 3.7, at the signal's path supposing a digital input from PC. The command signal is converted from digital to analog by the E-518 module, it passes through the E-509 control module , and finally through the amplifier module which produces as output the tension needed by the actuator to move as commanded. Signal is sent to the piezo device by means of the PZT port.

3.2.3.1 E-501 Module

As said in section 3.2.3, the E-501 is the chassis within which all the other modules are installed; on the rear face are placed the power supply plug, to which connect the alimentation cable to the electric socket, and an on-off switch. E-501 main features are reported in table 3.2, more detailed info are available in *PI E-501 datasheet* [11].

E-501 MAIN FEATURES	
Dimensions [mm]	236 x 132 x 296
Operating voltage [V]	90-120 / 220-264 V AC, 50-60 Hz
Max. power consumption [W]	80

Table 3.2: E-501 module main features

3.2.3.2 E-518 Module

The *PI E-518* module is the interface module to which is possible to connect the PC, it presents several ports which exploit different connection protocols. As visible in figure 3.8, the stage can be connected to the computer via USB, via RS-232 or via LAN cable (exploiting the TCP/IP protocol).
This electronic board includes three very important functions accessible via software: the wavegenerator function, the data recorder and the macro programming.
The wavegenerator is accessible via the *PI* software as a tool: it is possible, via graphics interface, to create a wave of desired shape, amplitude and frequency.

The data recorder writes files in *.dat* or *.csv* format, on which test features as time, actuator's voltage or position are available. The amount of data written on the file are limited by the module's volatile memory dimension; the sample rate is instead selectable until its maximum value (25 000Hz, or a value every 0.00004 seconds).
Macro programming gives to the user the possibility to send commands in GCS lenguage.
The PC can be connected using the *PI* software, which has graphics interface for the previous three functions, or writing an own software. The module, by means of installable drivers, is able to interface with sofware written in several environments: labVIEW, MATLAB, Visual Basic, Phyton, and all codes written in C, C#, C++.
A more detailed description is available in the *PI E-518 datasheet*

3.2.3.3 E-509.C1A Module

The servo controller module has the task to calculate and applicate the corrective action to the signal in order to reach the commanded position.
The stage, shown in figure 3.6, has an overflow led light, an on-off switch, a zero point adjustment screw, two ports to which connect the actuator and the sensor monitor plug.
The *overflow led* turns on if the input signal is near or exceeds the tension limits, T and P ports respectively refer to "target" signal and "probe" signal, the *zero* screw is a trim potentiometer which moves the zero point of the sensor. A calibration of the zero point is needed, for example, after long time operation because of changes in temperature which affect the performance of the module.
The *servo on-off* switch enables the control system to act on the command: if the servo is actived (servo on) the actuator will be commanded in *closed loop*, otherwise the actuator will move in *open loop*. In open loop mode (servo off) the user commands a tension, which moves the actuator in the correspondent position, in closed loop mode the user input is a position. Only using a software interface is possible to send a command position type to the actuator.
The *Sensor monitor* is a plug to which other electronic devices, such as an oscilloscope, can be connected. In this way it is possible to monitorate the

output to, for example, customize the proportional or the integrative term of the control system.
An integral description of the whole system is available in *PI E-509 datasheet*.
Let's take a closer look at the control system, visible in figure 3.8.

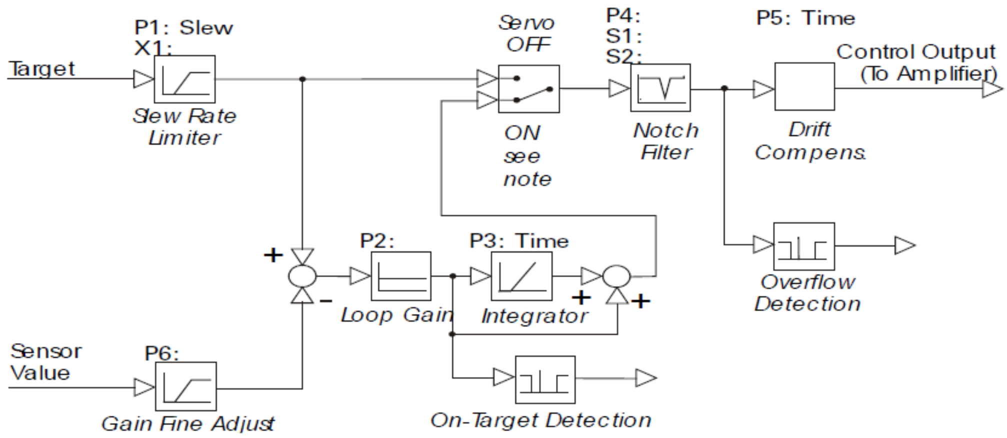

Figure 3.8: E-509 control system's logic [14]

As visible, it is a sort of proportional-integrative controller (P2,P3), with slew rate limiter, which provides a limitation of the command's slope; from the figure it's clear the function of the servo switch, if off position is setted the control system is fully bypassed. Signal passes then through a notch filter, which is a pass band filter, through a drift compenser and it is finally send to the amplifier stage, the *E-504.00F* module.

3.2.3.4 E-504.00F Module

The *PI E-504.00F* is the piezo amplifier module, it presents a led power light, which is green if the piezo controller module is on, a control input plug, a DC - OFFSET potentiometer and a PZT connector.
The *CONTROL INPUT* plug and the *DC-OFFSET* potentiometer serve to perform an analog control of the piezoelectric actuator. An external tension source can be connected to the plug while the potentiometer adds tension to the source's input signal, increasing the actuator's reachable position value.
The *PZT* is the port to which connect the actuator, this provides as output

the tension to make the piezo move.
In table 3.3 are shown the tension limits of the E-504.00F stage [12], a detalied description is available in the *PI E-504 datasheet*.

TENSION LIMITS STAGE E-504.00F	
Control input [V]	-2 to +12
DC - OFFSET [V]	0 to 10
PZT [V]	-30 to +130

Table 3.3: *E-504.00F* main features

It is possible to set the servo on, and so act in closed loop, also using the analog mode, in this way the position reached using tension as input is subjected to the control system.
For a complete description of the stage features read the amplifier module section in *PI E-500/E-501 datasheet*.

3.2.4 Sofwtare interface

The *PIMikroMove* software is the interface by which is possible to manage both the piezo controller module and the actuator. This code is suitable for simple applications, more articulated uses need a development of an own sofware.
The main *PIMikroMove*'s advantage is the graphic interface: for many available options the software provides easy access tools which doesn't require the knowledge of the GCS syntax, which is essential to modify non banal electronic boards options.
As said in section 3.2.3.2, installing the correct drivers, which are provided in the installation CD, it is possible to write code in environments as MATLAB, LABview, Phyton or others. However in this thesis the PI software will be used, a more detailed description will be given in chapter 5.

Chapter 4

Test Bench Development

This chapter's purpose is to provide a general description of the test bench used to analyze optic fibers' dynamic response.
The develpoment has been made considering some of the conclusions of the previous *Photonext* research works, in particular the optical fiber locking system. Fiber is fixed to two PLA or aluminum plates using epoxy resin [8].
The test bench is basically composed of a breadboard, several supports, plates and micro-positioners.

4.1 Breaboard

The *breadboard* is the table on which all the supports and plates are fixed by means of threaded holes; the one used in this thesis, visible in figure 4.1, is a honeycomb optical table produced by *NEWPORT* company.
The table 4.1 provides the NEWPORT's breadboard main features, more informations are available on the producer website.

Dimensions [mm]	900 x 900 x 58
Threaded Holes misure	M6
Holes distance [mm]	25
Work surface thick [mm]	4.8
Surface flatness	$\approx$ 0.1mm

Table 4.1: Newport's breadboard main features

Figure 4.1: Newport breadboard

The holed work surface is made of stainless steel, its production process, together with the table honeycomb structure, produces a highly damped feature.
If the breadboard's damping does not satisfy the user, it is possible to add some accessories to improve it: the easiest and cheapest solution is to install rubber vibration isolators. A bigger improvement is obtained using active vibration suppression systems, such as air compressed controlled structures, on which the breadboard is fixed. For this thesis the breadboard's damping is more than enough, so no vibration suppression accessories have been added.

4.2 Micro-positioners

The micro-positioner used in this thesis is a linear manual device, based on the nut-screw principle. It is composed of a rotary selector, on which is present a graduated scale, and a small surface which moves over two sledges once the selector is rotated.
It is possible to command a minimum displacement value of 0.01 mm while the maximum one is about 15 mm.
The movable surface has four M3 threaded holes through which is possible to fix little plates on which the fiber will be glued. Once the bonding is complete the user will be able to tensionate the fiber by acting on the selector.
Thanks to four through holes under the movable surface, the micro-positioner

can be fixed, by means of countersunk head screws, to an appropriate plate or support.
In figure 4.2 is shown the micro-positioner used, as visible is joined to an aluminium plate and over it a PLA plate is fixed.

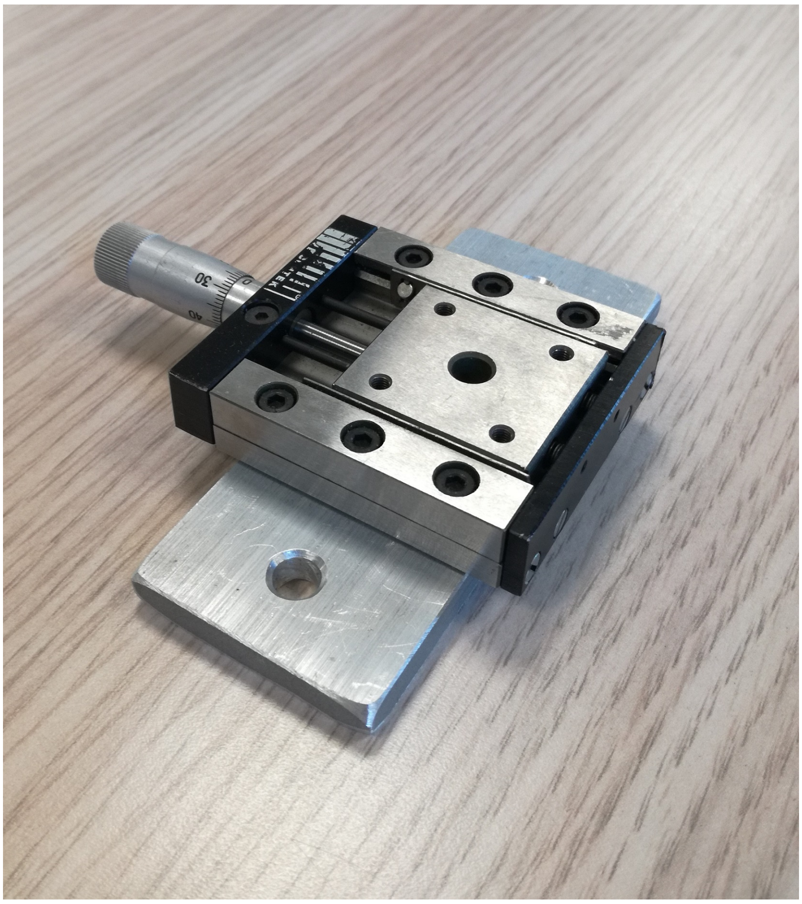

Figure 4.2: Micro-positioner on an aluminium plate

4.3 Supports and Plates: CAD design and main features

In this section are shown all the designed plates and supports with a brief description of their functions; only the main dimensions and features will be reported, for more details open the *Solidworks* parts and assembly designed file.

4.3.1 Breadboard to Piezoactuator Plate Connection - Support #1

It is an aluminium plate, bolted to the breadboard, on which is possible to fix the piezoactuator device. Four through holes allow M6 bolts to join the plate and the breadboard, four threaded holes allow the piezoactuator to be fixed to the plate.
Plate dimension and features are reported in table 4.2 while figure 4.3 shows the *Solidworks* support's design.

Dimensions [mm]	100 x 100 x 5
Threaded Holes misure	M3
Through Holes distance [mm]	75
Through Holes diameter [mm]	ϕ 6.6

Table 4.2: Breadboard to piezoactuator plate connection features

Threaded holes interaxis are taken from the *PI piezoactuator datasheet* [11].

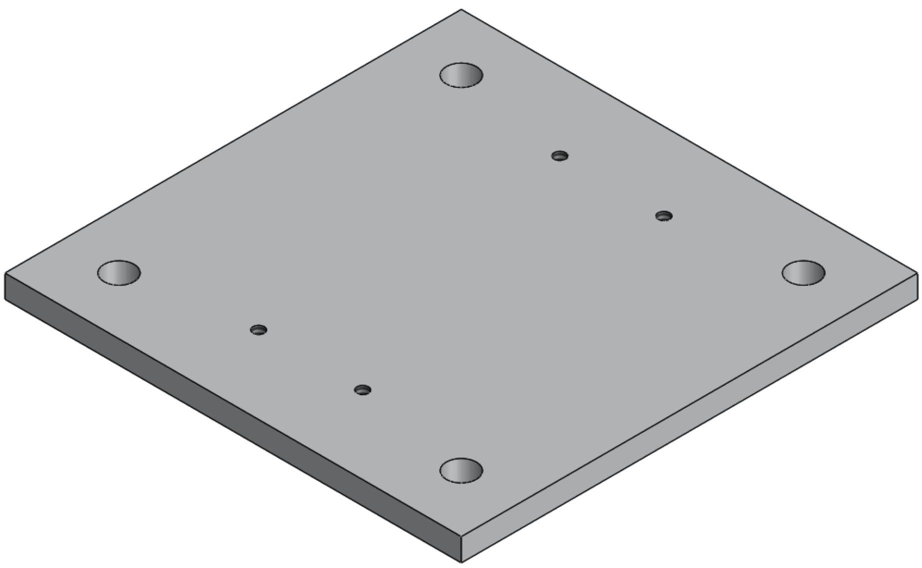

Figure 4.3: Aluminium breadboard to piezoactuator plate connection

4.3.2 Breadboard to Micro-positioner Plate Connection - Support #2

It is an aluminium plate, bolted to the breadboard, on which the micro-positioner is fixed. Two through holes allow the support to be joined with the breadboard while four threaded holes make the junction between micro-positioner and plate possible.
The plate *Solidworks* design is shown in figure 4.4 while its features are stored in table 4.3.

Dimensions [mm]	100 x 40 x 6.7
Threaded Holes misure	M3
Threaded Holes distance [mm]	20
Through Holes distance [mm]	75
Through Holes diameter [mm]	ϕ 6.6

Table 4.3: Breadboard to Piezoactuator plate connection features

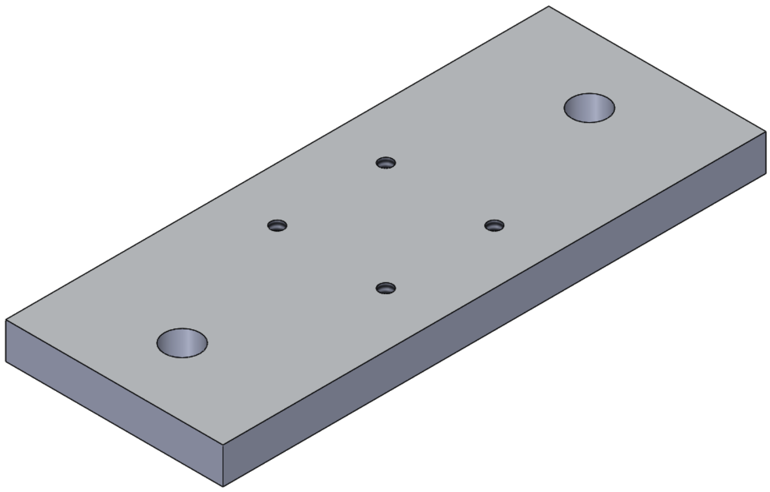

Figure 4.4: Aluminium breadboard to micro-positioner plate connection

4.3.3 Piezoactuator's Gluing Plate - Support #3

This is the plate on which the fiber is glued. The dimensions and the holes interaxis are equal to the actuator ones, taken from the *PI LISA actuator*

datasheet, over which this support is fixed. It has been designed with different thicknesses, to verify the influence of the plate's mass on the dynamic response, and materials, to verify the stiffness material's influence on the analysis. Initially PLA 3D printed plates have been used then aluminium ones have been chosen.
In figure 4.5 is shown the *Solidworks* design while the features are reported in table 4.4.

Dimensions [mm]	73.5 x 16
Thickness [mm]	2 - 3 - 5
Through Holes distance [mm]	25 horizontal - 10 vertical
Through Holes diameter [mm]	ϕ 2.90

Table 4.4: Piezoelectric actuator gluing plate features

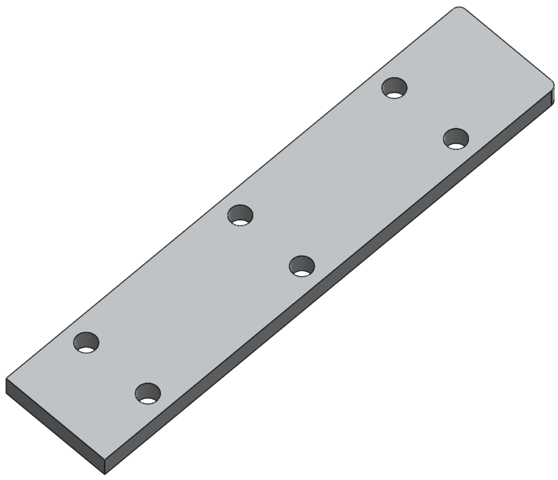

Figure 4.5: Piezoelectric actuator gluing plate

4.3.4 Micro-positioner's Gluing Plate - Support #4

This is the second gluing plate, joined to the micro-positioner's movable surface. Since that no datasheet of the micro-positioner is available, the support has been designed measuring the movable surface's dimensions.
The support, as the actuator gluing plate, has been produced with different

materials, first PLA and then aluminium, and thickness dimension.
Figure 4.6 shows the micro-positioner's gluing plate while table 4.5 shows its feature.

Dimensions [mm]	32 x 28
Thickness [mm]	2 - 3 - 5
Through Holes distance [mm]	20
Through Holes diameter [mm]	ϕ 3.40

Table 4.5: Micro-positioner gluing plate features

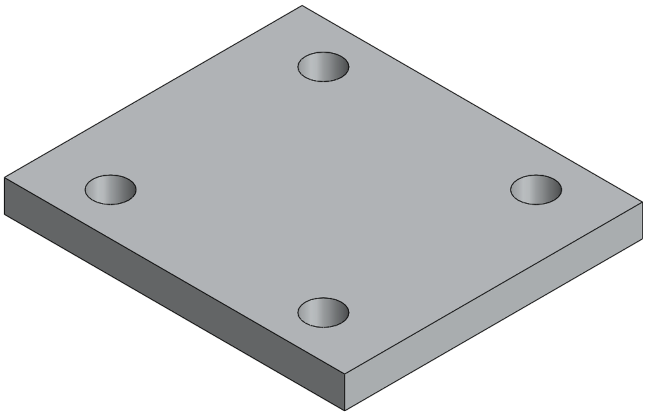

Figure 4.6: Micro-positioner gluing plate

4.3.5 Gluing Support Turret - Support #5

These supports have been designed to achieve a better fiber's bonding procedure result, their function is to mantain the planarity of the gluing stage. A more detailed description of their function will be given in section ... .
As that the thickness of the gluing plates is variable, the support turrets have been designed in two pieces: a base and some plates, in turn of different thickness, which have to be installed one on the other.
Each gluing station needs two turrets which are placed one behind the actuator and one behind the micro-positioner. The turrets have four through holes, M6 bolts are used to fix them to the breadboard while the fiber is fastened on them with adhesive tape.

The *Solidworks* pieces' design is shown in figure 4.7 while their features are listed in table 4.6.

Dimensions [mm]	40 x 40
Plate Thickness [mm]	2 - 3 - 5
Turret Thickness [mm]	20
Through Holes distance [mm]	25
Through Holes diameter [mm]	ϕ 6.60

Table 4.6: Turret support pieces features

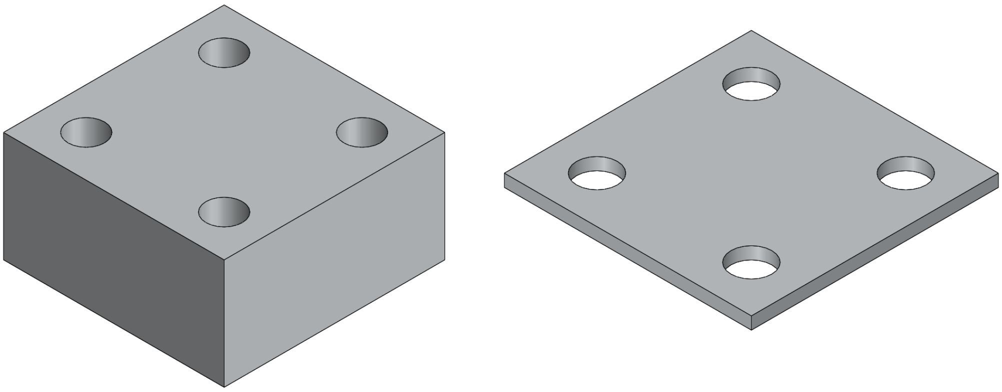

Figure 4.7: Turret support pieces

4.3.6 Piezoactuator Similar Device - Support #6

In order to have a second gluing station, a piezo-actuator look alike device has been designed. This support has been 3D printed in PLA, considering that the printer has not a sufficiently high precision to print a threaded hole and the PLA is not suitable to be threaded, an alternative solution has been realized. On the top surface of the device, six exagonal seats of the dimension of M2.5 nuts have been obtained, the nuts have been inserted in these, allowing in this way to fix the actuator's gluing plate (support #3) on it without clearance.
As the original device, it has four M3 through holes, bolts are used to fix it to the support #1. The holes interaxis have been taken in the *PI LISA*

datasheet.
The *Solidworks* design is shown in figure 4.8 while its dimensions are listed in table 4.7.

Dimensions [mm]	80 x 36 x 15
Seat length [mm]	5.1
Seat dept [mm]	5

Table 4.7: Piezo similar device features

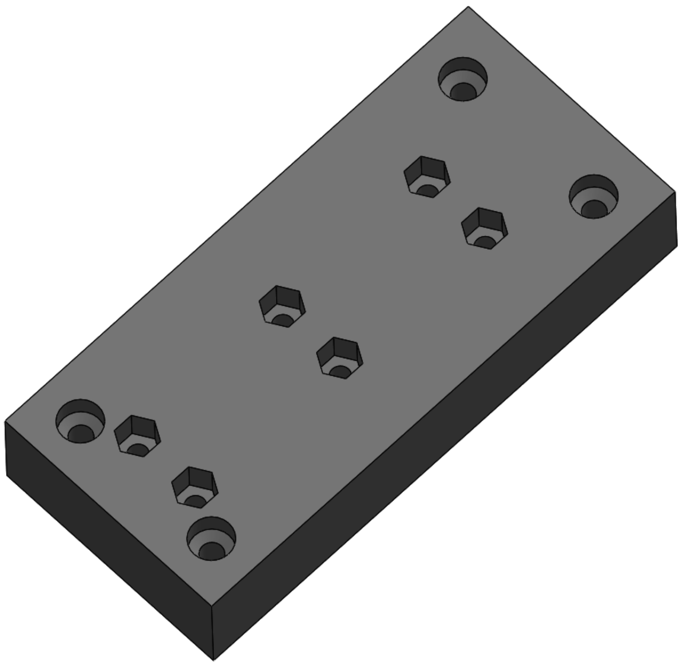

Figure 4.8: PLA actuator look alike device

4.4 Assembly of the Supports

Combining all the supports showed in section 4.3, it is possible to obtain the simpliest configuration to analyze the fiber's dynamic response, this will be descripted in detail in the following section.
The test bench consists of two main assemblies: the actuator one and the

micro-positioner one.
The actuator's assembly is composed of:

- the breadboard to piezoactuator plate, support #1;
- the piezoelectric actuator, or the similar support #6;
- the piezoactuator's gluing plate, support #3;
- one gluing support turret, support #5.

As visible in figure 4.9, the support #3 is joined to the actuator, or the similar support #6, which is fixed to the aluminium plate; the support #1 is then bolted to the breadboard and behind this group is placed the gluing turret.

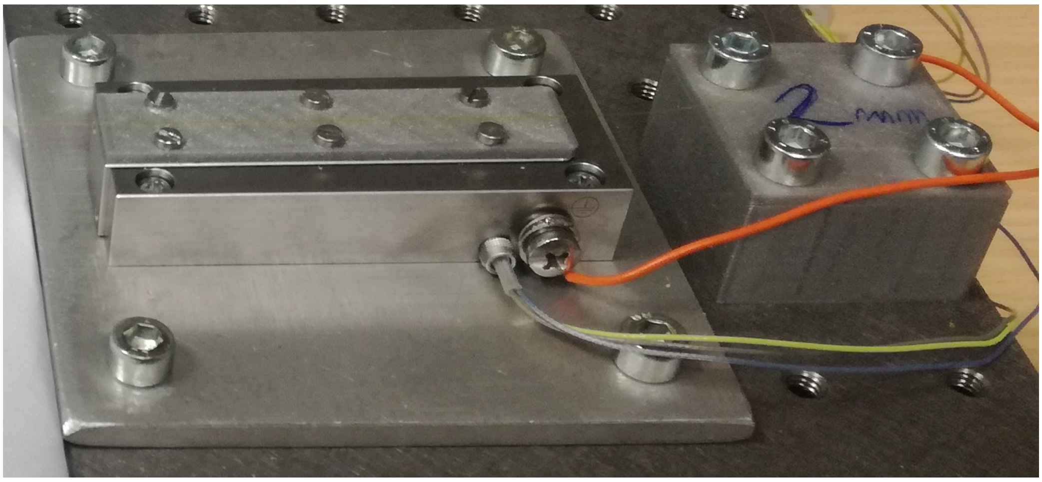

Figure 4.9: Actuator assembly

The micro-positioner's assembly is composed of:

- the breadboard to micro-positioner plate, support #2;
- the micro-positioner;
- the micro-positioner's gluing plate, support#4;
- one gluing support turret, support #5.

In figure 4.9 is shown the second assembly, the support #4 is fixed to the micro-positioner which is bolted to the aluminium plate; the support #2 is then connected to the breadboard and behind this group is placed the gluing turret.

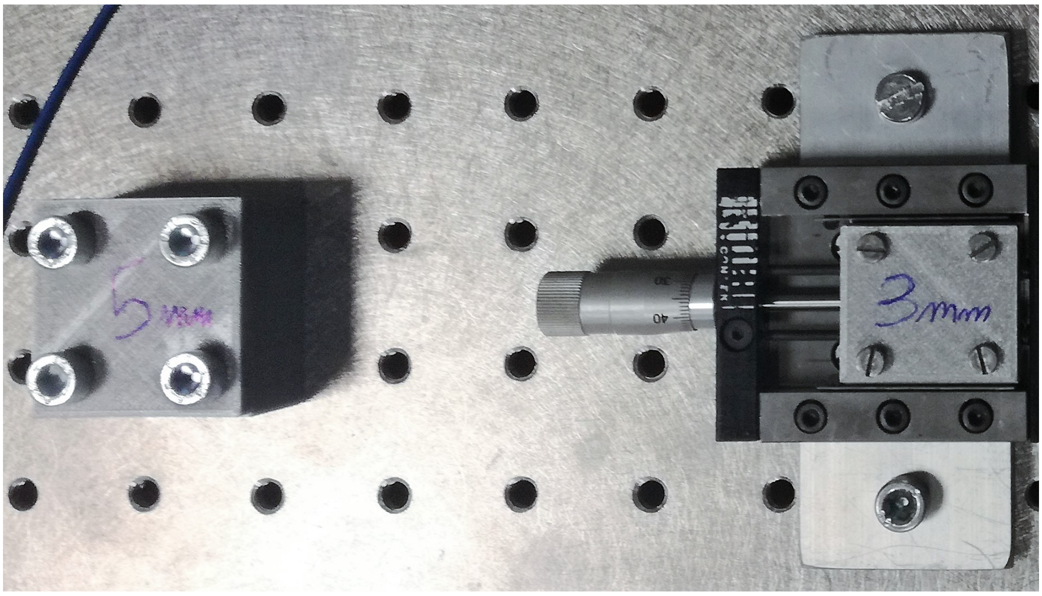

Figure 4.10: Micro-positioner assembly

These two assemblies must be mounted at a precise distance selected by the user, the distance between the two assemblies' gluing plates is the *effective fiber length* , this is the element which mainly determines the behaviour of the fiber.
Once that the two assemblies are fixed to the breadboard, the fiber gluing procedure can be made. The fiber has to be glued with the Bragg sensor between the two plates, only in this way the FBG will be able to provide the deformation values to which the fiber is subjected.
In order to obtain the best process' performances some little precautions must be taken. Before starting the process it is really important to clean the gluing surfaces with alcohol, this will maximize the bonding between plates and fiber. During the gluing procedure, only a thin layer of resin must be applied, excessive quantities of glue may influence the measurements. Moreover, is reccomended to apply a little pre-tension during the procedure, holding the fiber to the turrets with adesive tape.

The gluing process lasts from 12 to 24 hours, this period is necessary to obtain a solid bonding. In the first hours the epoxy resin is not hardened: every movement on the fiber will result in a position error at the end of the bonding process. While vertical displacement are prevented by vinculating the fiber to the two turrets, the other ones are totally unprotected: they are avoidable only if the fiber is not touched or displaced during all the hardening period.
In figure 4.11 is shown the test bench setup with the actuator, figure 4.12 shows the second gluing station with actuator similar device.

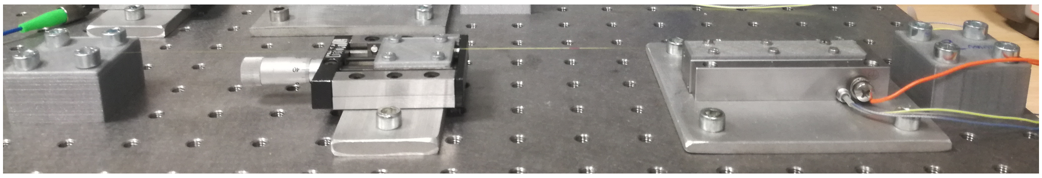

Figure 4.11: Test bench configuration

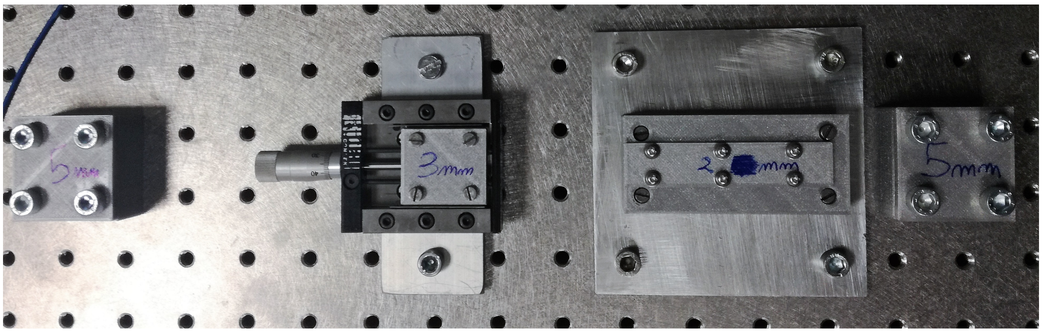

Figure 4.12: Second gluing station

4.5 Complete Test Bench Setup

To complete the test bench setup all that remains is to connect the fiber to the interrogator, once the gluing procedure is over, and the piezoelectric actuator to its controller. Controller and interragator are then connected to the PCs, started on and commanded by their software via PC, or, considering the piezo controller, by means of other device as the tension wavegenerator. Figure 4.13 shows the complete test bench setup, on the piezo controller is visible the tension wavegenerator for controller analog input mode, in this case the *PIMikroMove* software is used only as data recorder. A more detailed software description will be given in the successive chapter.

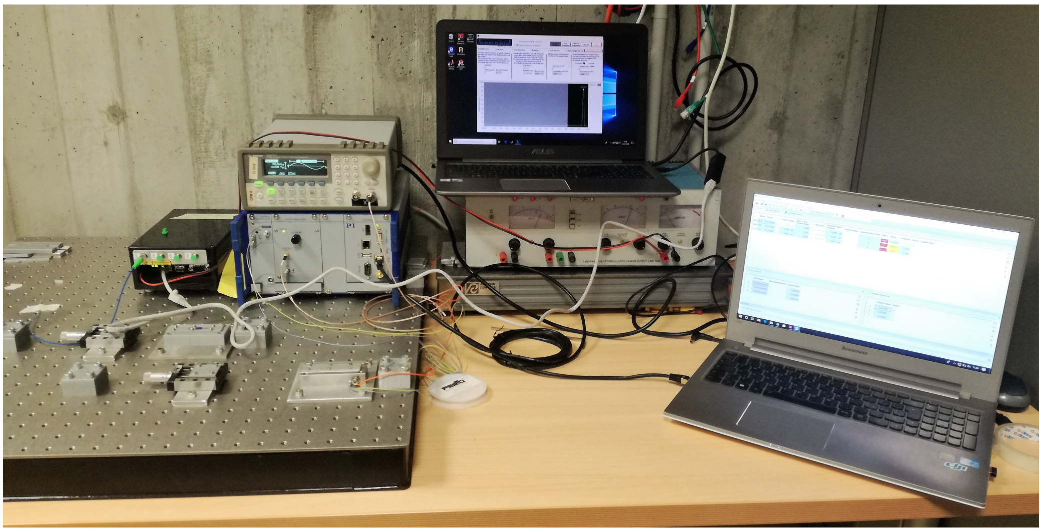

Figure 4.13: Test bench complete setup

The two computers visible in the figure have been used only to speed up the measurement operations, all the analysis can be conducted using only one.

Chapter 5

Software and MATLAB Script Description

In this chapter the interrogator software, *SmartSoft SSI 4.1.1*, the piezo controller sofware, *PIMikroMove* and the MATLAB script written to process the data will be descripted more in detail.

5.1 SmartSoftSSI 4.1.1

The interrogator model used in this thesis is not the same used in the previous *Photonext* research works, a different software release is then necessary. The software compatible with the *SmartScan SBI* is the *SmarSoftSSI 4.1.1*, which has the same functions and the same graphic interface of the *3.2.0* version. The old one is not suitable to this model because of different connection drivers.
The first step to accomplish is the PC-interrogator connection, once the interrogator is started on and connected via LAN cable to the PC it is possible to open the software. Opening the software will produce a connection window, visible in figure 5.1, in which the standard IP address of the interrogator will be shown. By clicking "ok" the connection will be enabled, if the connection time is too long is necessary to change the corrispondent IP address of the PC, usually the address 10.0.0.2 allows the connection.

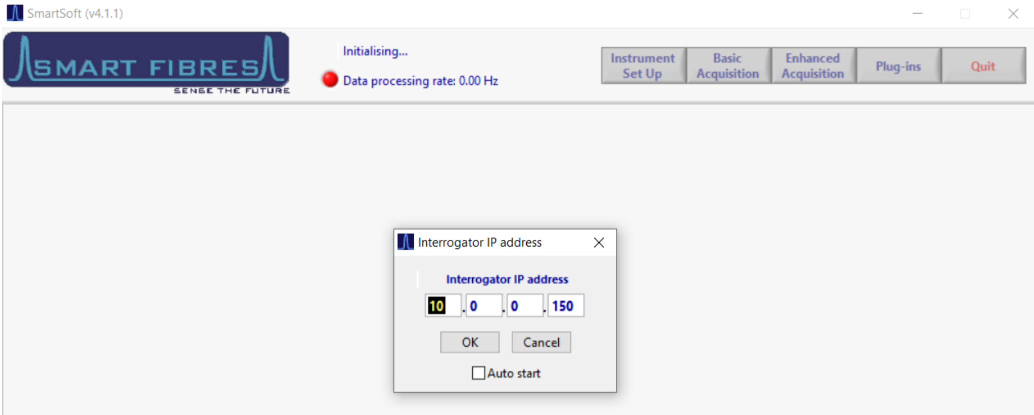

Figure 5.1: SmartSoftSSi 4.1.1 connecting windows

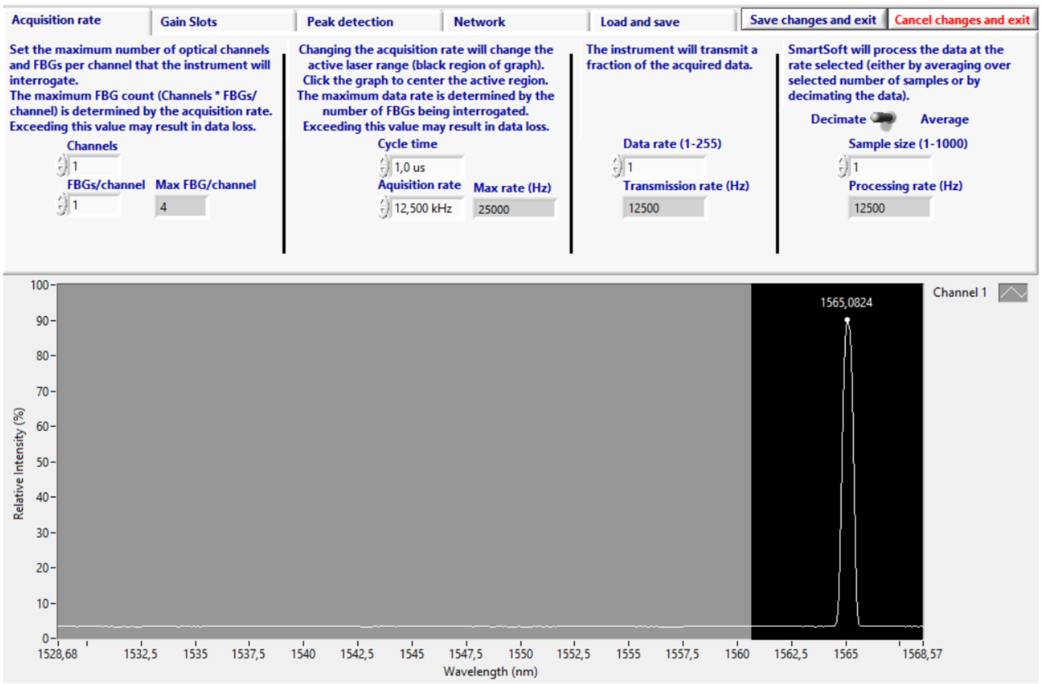

Figure 5.2: SmartSoftSSi 4.1.1

Once the interrogator is connected, software interface comes as in figure 5.2. In the upper part of the window there are four selectable options.
The first one, starting on the left, gives to the user the possibility to choose which channels and how many Bragg sensors to interrogate. The measure of the chosen channels and Bragg sensors will be plotted on the graphic in the lower part of the window.
The second option gives to the user the possibility to choose the interrogator work frequency and the duration of the process in which the laser beam is sent, received and processed by the interrogator itself. Frequency has to be selected keeping in mind the Nyquist theorem: to avoid aliasing it is necessary to choose the interrogator frequency about ten times greater than the frequency of the phenomenon.
In this thesis the actuator frequency range is from 0 to 1000 Hz so at least an interrogator working frequency of 10 000 Hz has to be set, 12 500 Hz has been chosen for all the analysis.
The third option is used to transmit a fraction of the acquired data, setting 1 as value all the data will be trasmitted. Value has been set to 1 for all the analysis.
The fourth option concerns the data processing and their writing in an output file. A number from 1 to 1000 can be set, if 1 is set all the data will be processed and written in the file, with every other number n only one measure every n will be written. A value of 1 has been set for all the analysis.
Once that the interrogator work options have been set it is possible to start the data recording.
Two options are available, *Basic Acquisition* which records the Bragg sensors wavelength variations, or *Enhanced acquisition* on which is possible to specify what type of sensors are the FBGs interrogated. Temperature, strain, pressure and wavelength are selectable options. In this thesis a basic acquisition has been used for all the analysis, so wavelength has been transformed through the MATLAB scripts into the desired physical quantities.
Figure 5.3 shows the *Basic acqusition* window. Before starting a registration it is necessary to provide the destination, where the file is going to be saved, and the output file name, writing them in the blank subwindow. Clicking on "Log" button the recording will be started, clicking again on "Log" the recording will be stopped. It is possible to select an exact duration of the

registration by selecting the desired time in the "Log time" subwindow.

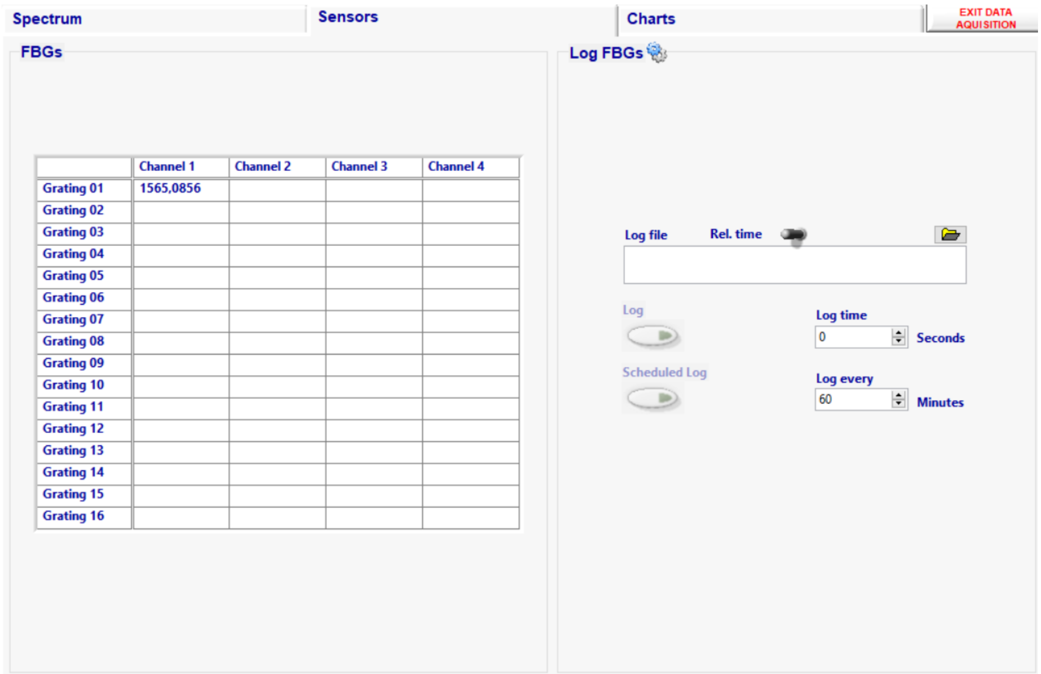

Figure 5.3: SmartSoftSSi 4.1.1 basic acqusition window

The ouptut file will be saved as a *.log* file, a sort of text file which can be easily read by MATLAB.
Many other options are customizable, for a complete software description consult the *SmartSoft v4.1 User Manual* [16].

5.2 PIMikroMove

This is the software, developed by *PI*, used to control and command the piezo controller module and the piezoelectric actuator.
Opened the software, with the control unit connected to the PC, a connection window will automatically generate (figure 5.4): the window requests to select the interface module, in this case E-518, and the protocol connection, USB or LAN.
Once connected, the software graphic interface comes as in figure 5.5.

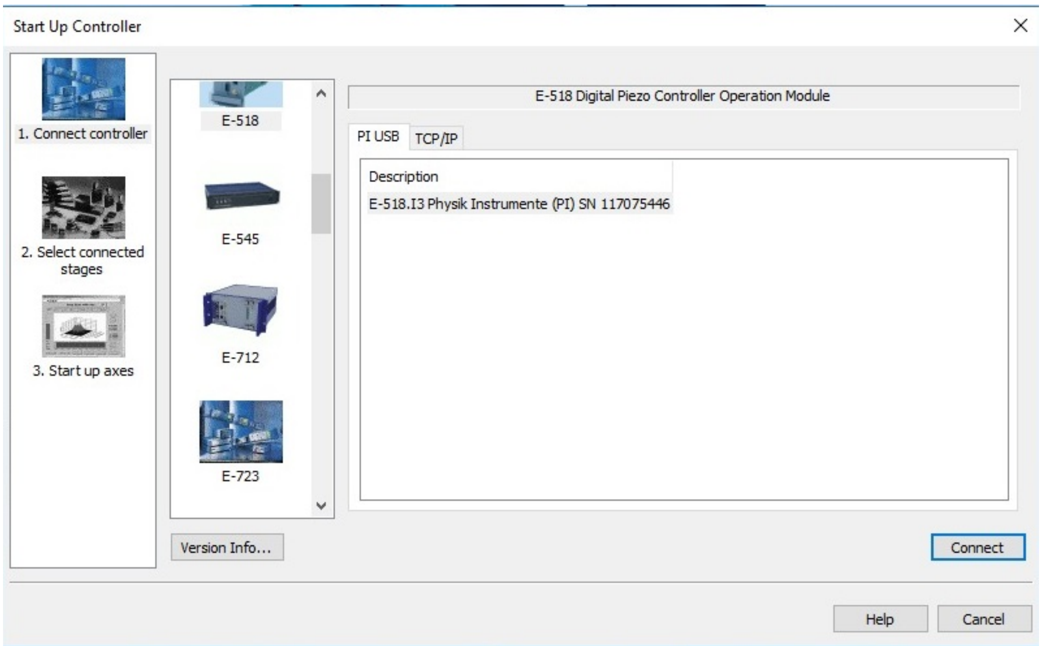

Figure 5.4: *PIMikroMove* connection window

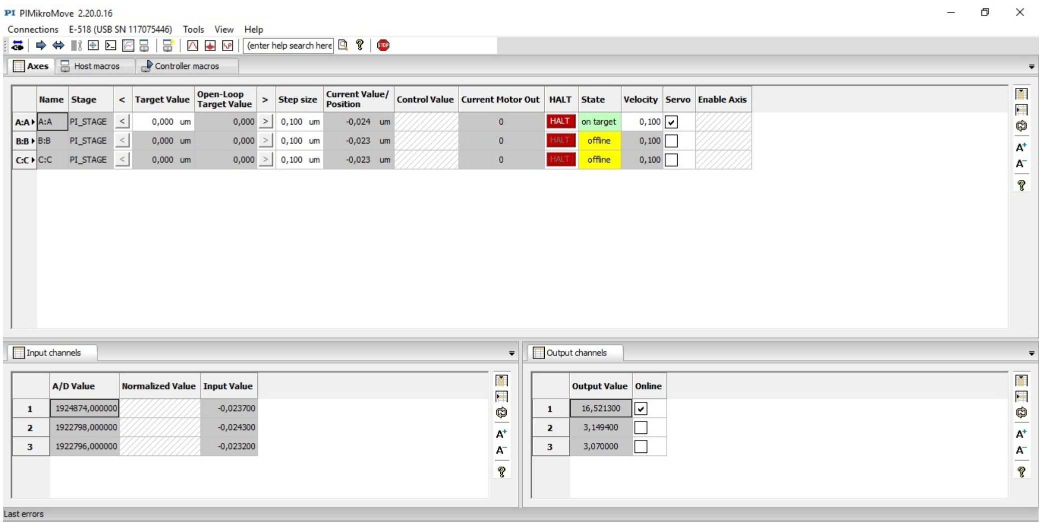

Figure 5.5: *PIMikroMove* window

In the upper part of the window are shown three rows which correspond to the maximum number of actuator that can be managed from the software. The E-509.C1A module allows only the connection of one actuator, so only the first row of the software will be active. The active rows, and so the relative actuators, are indicated by a green cell with "on target" write on it. The "Servo" cell, if checked, enable the control in closed loop; in the "Target" cell it is possible to write an input value: if the servo switch is on, or the "Servo" is selected, the value commanded will correspond to a displacement in μm, otherwise it will command a voltage.
By clicking "E-518" in the top bar of the software window many functions and tools are available, only two has been used: the *Wavegenerator tool* and the *Data recorder tool*.

5.2.1 Wavegenerator Tool

Opened the tool, the graphic interface displayed is shown in figure 5.6.

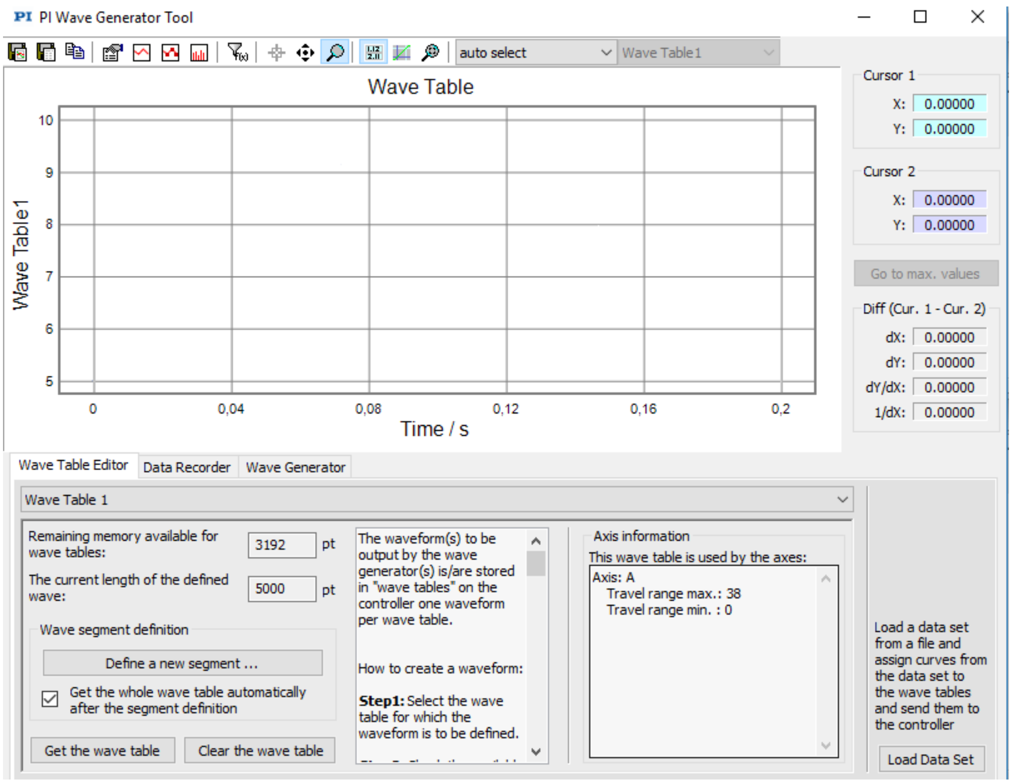

Figure 5.6: *PIMikroMove* wavegenerator tool

By clicking "Define a new segment" it is possible to create the wave of the desired shape. Figure 5.7 shows the control parameters to define the wave.

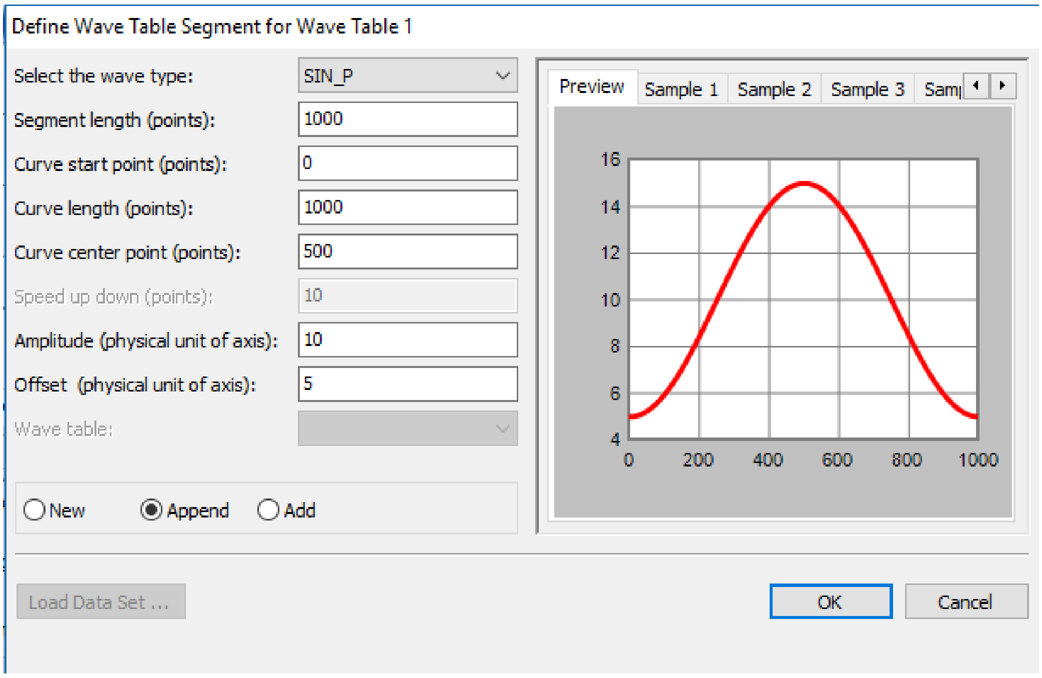

Figure 5.7: *PIMikroMove* wavegenerator tool, wave definition

To generate a wave, first of all, it is necessary to choose the waveforms that are stored in wave tables on the controller. Depending on the controller, different wave forms are available: ramp, sinusoidal and others. In this thesis the sinusoidal wave, stored in SIN_P table, has been chosen.
Once selected the wave form, the other wave features must be set: frequency, offset and amplitude. Offset and amplitude unit of measure is μm, regarding the frequency it is necessary to explain the tool's working logic.
As visible it is not possible to insert the frequency directly in Hz, this because the controller works by points: to obtain a determinate frequency, it is necessary to calculate its number of points. The wavegenerator tool works on an electronic board of finite dimension, in particular it can store only 8192 points. At each point corresponds a time value, the minimum distance between two points is 0.00004 seconds. It is clear that the maximum period available is

$$8192 \cdot 0.00004 = 0.3277\ s$$

To which corresponds the minimum frequency of 3.517 Hz.
The "curve center point" is the point on which the maximum value will be reached, to obtain a perfect sinusoidal wave this point has to be exactly the half of the "curve length" value.
Selecting the "New" box, a new wave with the inserted features will be generated; by selecting "Append" another wave with the same features will be concatenated to the first one, if enough free memory is available. The "appended" waves are always an entire number, this means that if in the memory there is no enough space for another entire wave, no partial wave is added to the concatenated ones[1].
After the wave is generated, it will appear in the tool as in figure 5.8.

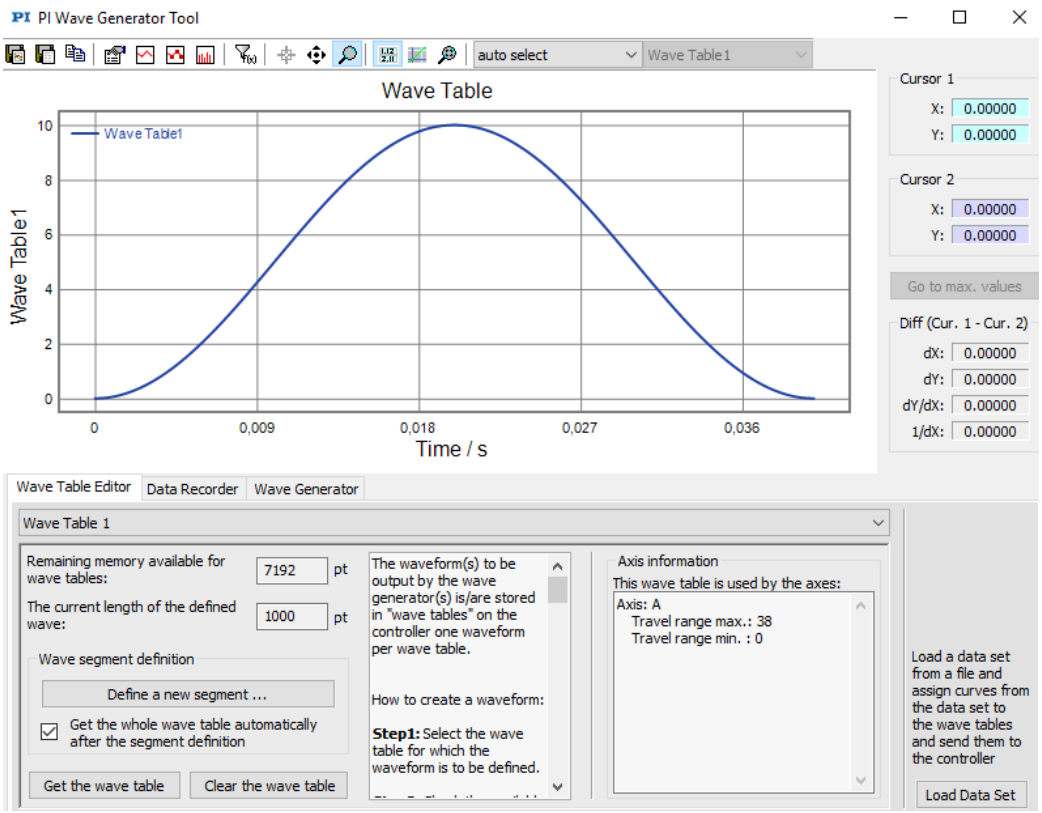

Figure 5.8: Example of sinusoidal wave

As visible a data recorder is already integrated in the wavegenerator window,

[1] An example makes all easier: supposing a 1000 points wave, a maximum of seven waves can be added, composing a total of 8 waves, filling 8000 points out of 8192 available.

it is possible to access it by clicking the "Data Recorder" by which is possible to: display the data, modify the physical quantities recordable (tension or position), the record starting point or the record rate.
As the Wave Table Editor, also the amount of recordable data is limited by the size of the controller's finite memory: the maximum number of cells storable is 8192, so only 0.3277 seconds can be registered.
To overcome this limit it is possible to modify the "Record Table Rate": varying this value with a n entire number, only a point every n will be plotted[2] and a longer time of the test is then recorded. It is necessary to be carefull with the "Record Table Rate" value, if the frequency of the wave and the sample time are similar, aliasing may occur. Nyquist theorem must always be respected[3].

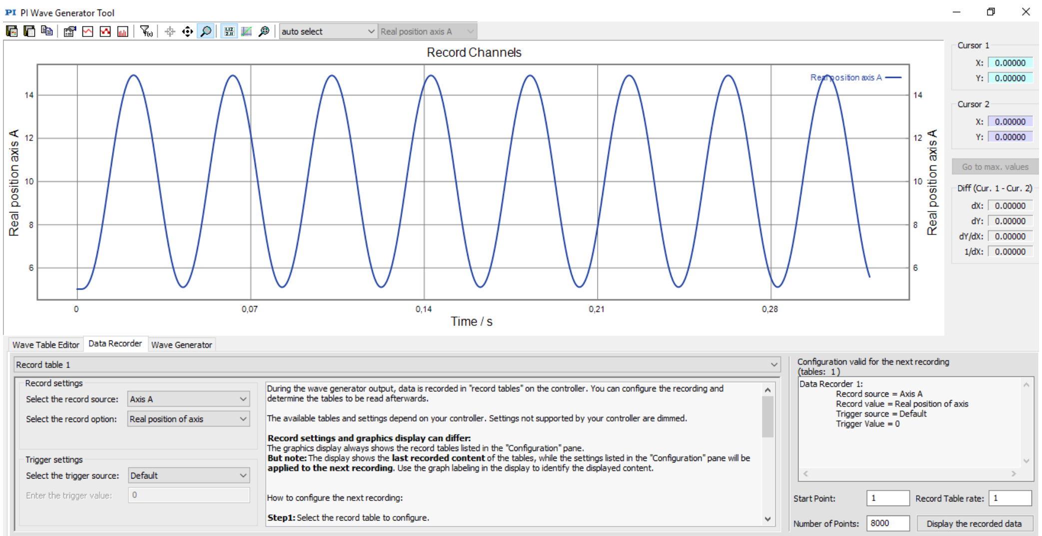

Figure 5.9: Data recorder options

By clicking "Wave Generator" (figure 5.10), it will be possible to set the duration of the test the "Number of Cycles" option. Setting "0" the actuator will be manually started and manually stopped with their buttons. Otherwise an

[2]The standard rate (record rate = 1) plots a point every 0.00004 seconds, setting n will plot a point every $n \cdot 0.00004 seconds$.

[3]For example, a table rate of 16 means a point every 0.00064 seconds, frequency of hundred of Hz may suffer the aliasing, the sample time - wave period ratio is no more 10:1.

entire number n must be set to produce a duration of $n \cdot wave\ period\ [s]$ or $n \cdot wavecycle\ period\ [s]$[4].
To facilitate the user, a MATLAB script which calculates the number of points of the desired frequency, the maximum number of addible waves and the number of cycles required to produce a determinate duration has been written[5].

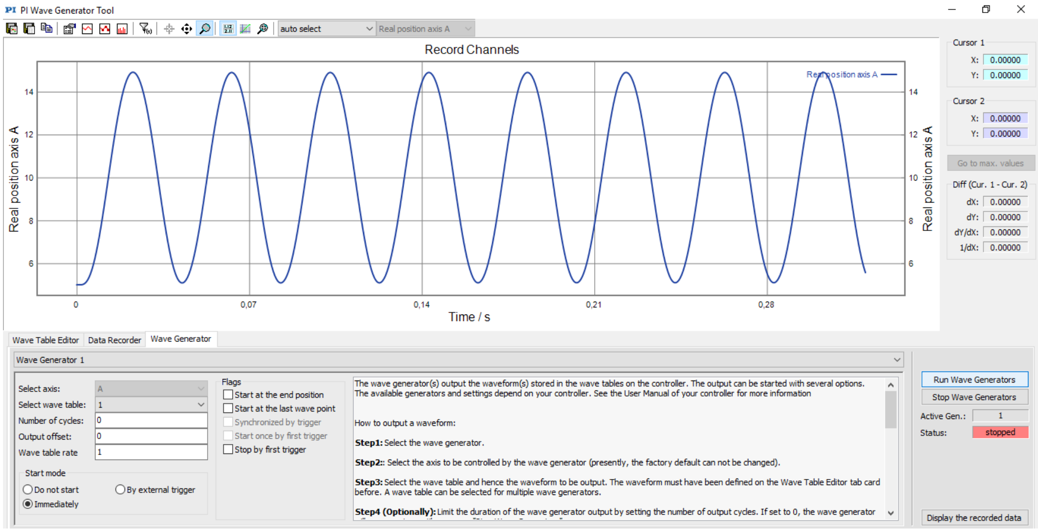

Figure 5.10: Wave generator options

Both "Data Recorder" and "Wave Generator" option give the possibility to save the recorded data and the image produced. Data can be saved in two different formats, *.dat* file or *.csv* file, a type of Excel extension. The output file has to be saved as *.csv* file in order to be readable from the written MATLAB scripts.
A big limitation of the tool is the necessity to provide the wave features by points, this produces a strong lack: working only with entire number of points some frequencies won't be available. For example 70 Hz will not be available, the nearest frequency is 70.28 Hz.
The other big limitation is the amount of data storable, once that the 8192 cells are filled the controller won't record anything of what will happen later.

[4] for a detailed description see 5.3.1.1
[5] *calcolo_frequenza_punti.m*

The available data will be only from 0 to 0.3277 seconds. A more detailed description is given in the *PIMikroMove Software Manual* [17].

5.2.2 Data Recorder Tool

The "Data Recorder Tool" is used to record tests made with the actuator controlled in analogical way, as explained in section 3.2.3 , or to register step and impulse command.

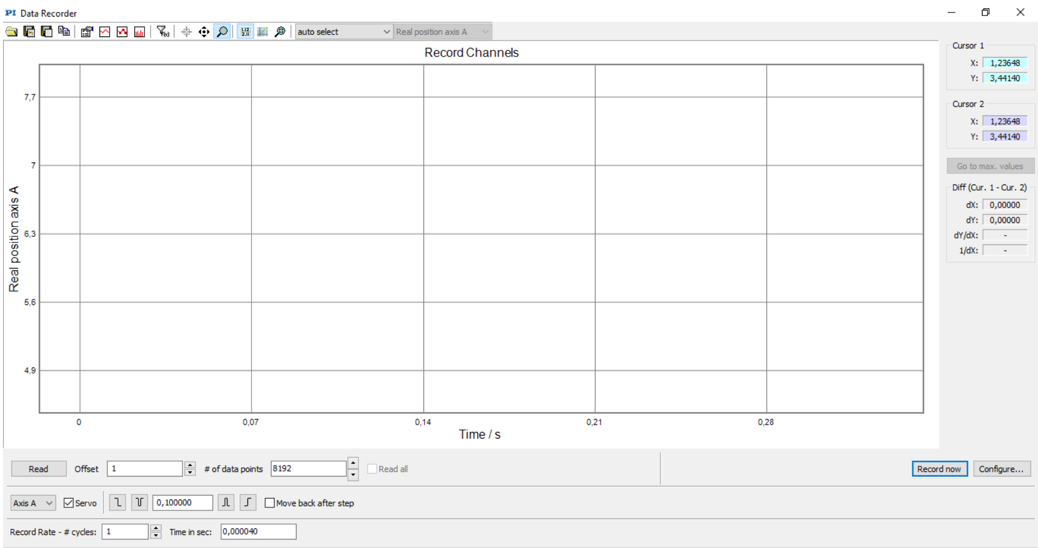

Figure 5.11: Data Recorder Tool window

Figure 5.11 shows the available options of the tool, it is possible to: record the test by clicking "Record Now", modify the "Record Table Rate" value, select the duration of the record by choosing the number of cells (from 1 to 8192), give a step or impulse command of amplitude desired.

Results can be exported and saved in the same format of the wavegenerator tool.

A more detailed description is given in the *PIMikroMove Software Manual* [17].

5.3 MATLAB scripts

Once that the tests have been done and recorded by both the interrogator and the controller, the output files must be compared to analyze the fiber behaviour under the actuator's input. In order to make the scripts work, the interrogator sample rate must be set to 12 500 Hz while the controller record rate must be set to 1 (sample rate 25 000 Hz).
All the scripts have been written with the purpose of provide as results the Bode diagram of the fiber, which is the main result of a dynamic analysis or a frequency response.
Two programs have been developed: the first one, *Analisi_dinamica.m*, produces the amplitudes' ratio between what registered from the interrogator and what provided by the actuator at a selected frequency; the second one, *Diagramma_bode_sperimentale.m*, after several frequencies have been tested, provides the Bode diagram of the fiber.

5.3.1 SCRIPT Analisi dinamica.m

Analisi_dinamica.m is a script which is composed itself by other MATLAB program. Once run, in the command window will appear the instructions to correctly use the program.

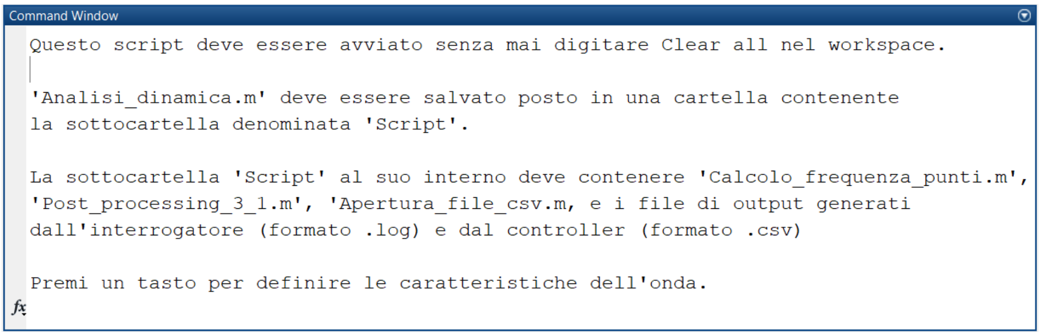

Figure 5.12: Main *Analisi_dinamica.m* instructions

All the scripts needed to make the program working are already included in the *Script* folder. The output file of both the interrogator and the controller has to be manually added to this folder. After the program is run no "clear

all" command must be sent.
Sections 5.3.1.1, 5.3.1.2, 5.3.1.2, explain the script run externally by *Analisi_dinamica.m*, section 5.3.1.4 explains the core of the code written in *Analisi_dinamica.m*.

5.3.1.1 Calcolo frequenza punti.m

This script simplifies the user work, providing as output the wave frequency in number of points and the test duration in number of cycles.
As said in section 5.2.1, the controller's working logic limits the frequency available, when the wave frequency is inserted, the program may respond in two ways:

- if the frequency selected produces a non entire number of points and it is far from the one desired, the script will display an error, indicating which is the nearest frequency respect to the one inserted, and will re-ask the user to insert a valid one;
- if the frequency inserted produces a non entire number of points but the one available is near (< 1 Hz) to the desired one, the program warns the user that it will continue with the available frequency , displaying how much it is far from the inserted one.

Once the frequency is correctly inserted, the script will request to insert the "number of concatenated wave"[6] and the duration of the test, returning as output the "number of cycle" to make a test of the desired duration.
The number of waves concatenated influences directly the calculation of the "number of cycle". The value inserted as number of concatenated waves will compose the "wave cycle", for example if the user sets a value of concatenated waves of 5, every wave cycle will be composed by 5 waves and its period will be the sum of the 5 single wave periods. A number of cycle of, for example, 10 in this case will imply a duration of $10 \cdot \textit{wave cycle period}$ so 50 times the period of the single wave. These two parameters will be of fundamental importance for the real *Analisi_dinamica.m* code.
The wave characteristics inserted in the MATLAB script must be exactly the same that will be inserted in the wave generator tool, otherwise error or no sense results may be produced.
After that data loading is complete, post processing can be started.

[6] See section 5.2.1, Append option.

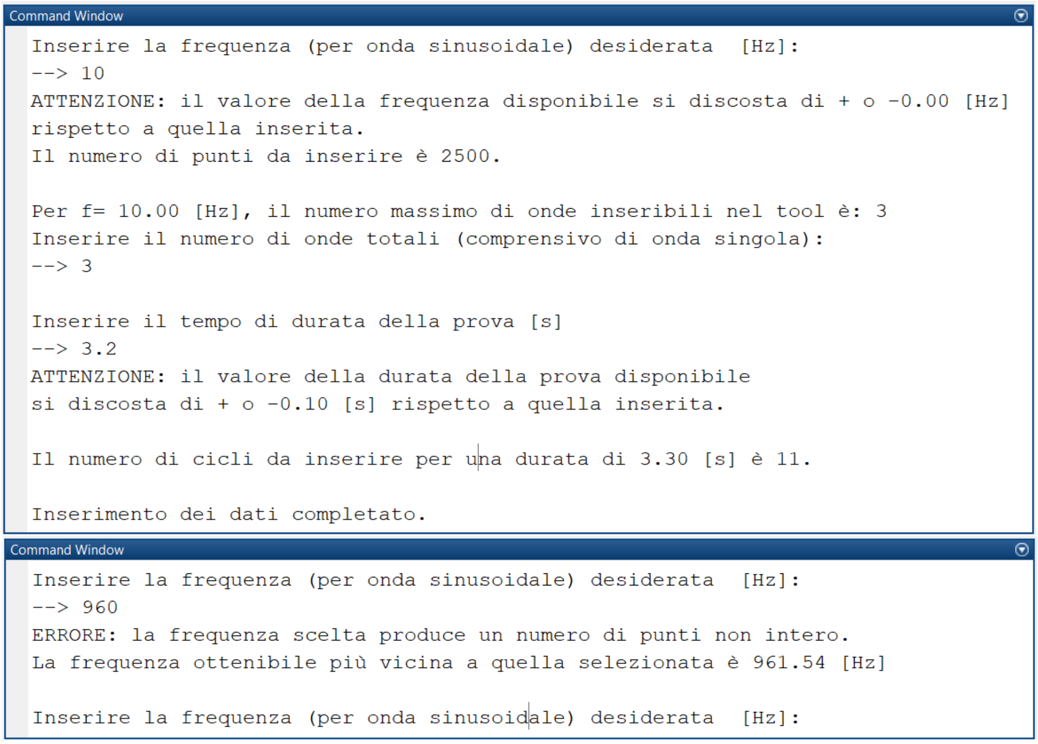

Figure 5.13: *Calcolo_frequenza_punti* possible scenarios

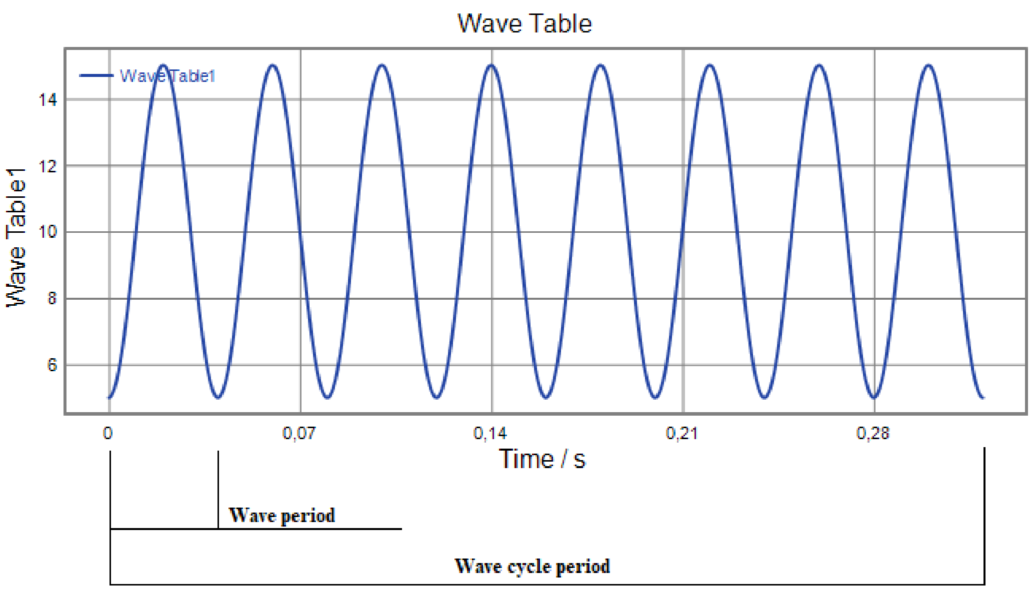

Figure 5.14: Wave period and wave cycle period

5.3.1.2 Post processing 3.1.m

This is a revisitation of the script *post_processing_3_0.m* described in the previous *Photonext* reasearch works, in particular in [15]. The core of the program is the same, but the not necessary parts for this type of analysis have been removed, making it faster and simplier.
The first thing the script requires is the name of the interrogator output file that the user wants to load, which has to be manually added to the "Script" folder. Inserted the name of the file, the program will load the data and will ask the user if he wants to write a comment. Then it will give the possiblity to set manually the fiber's parameters and the wavelength at rest or set them automatically. For last it will ask if the set wavelength characterizes the strain of the fiber or the temperature. This script provides as result a vector of values in microstrain, starting from the fiber's wavelengths data available on the file.

5.3.1.3 Apertura file csv.m

This program loads the controller output file, in format *.csv*, which contains the actuator's data of the test: time and its relative position and voltage.
The output file must be manually inserted in the "Script" folder. Once started it only requires to the user to insert the name of the file, comprehensive of the *.csv* extension, the script will load the available data and will memorize them into variables.

5.3.1.4 Analisi dinamica.m code

The script has now loaded and memorized in variables the data of both fiber and actuator; the other parts of the code will calculate and display the fiber - actuator amplitude ratio.
A description of the code's working logic is here given. First of all the code verifies that the test has been done by starting the interrogator before the piezoelectric actuator, otherwise it will be necessary to repeat the measure respecting the correct order.
It is clear that the time instant in which the interrogator record begins and the instant in which the actuator starts to move will not be the same, the

code will detect on the interrogator measure where the test starts, memorizing its cell.
From this cell, in order to have a perfect match between the sampling frequencies of both the controller and the interrogator, a cell every 2 on the controller file has to be eliminated, a time interval of 0.00008 seconds is obtained for both the two output files. In this way the peaks of the actuator's position not detected by the interrogator, due to its hardware limits, are eliminated and a more precise ratio will be obtained.
The code will work parallely on the vectors memorized and processed from the two ouptut files so, for an easier comprehension, a separated description of the two set of variables may be made.

Vectors from interrogator output files and post processed.
The data on which the code will operate, will be the fiber microstrain vector computated by the *Post_processing_3_1.m*.
Considering the value of the "number of cycle"[7] 3 scenarios may occour:

- The "number of cycle" n is $>= 3$, from the starting cell the code will detect the penultimate "wave cycle". All the cells before the start of penultimate wave cycle and the cells after the ending point will be deleted;
- the "number of cycle" n is $= 2$, from the starting cell the code will detect the second, and last, wave cycle. It eliminates all the cells before the start of the ultimate cycle and all the cells after the ending point;
- the "number of cycle" n is $= 1$, the code will eliminate all the cells before the starting point and all the cells after the ending point.

Using a "number of cycle" > 3 it will be possible to avoid transitory effects, as overshoot, and take fiber's values when they will be stable.
Once selected the effective data on which acting, the code will research the maximum and the minimum values of this cycle.
This is where comes into play the "wave cycle" value:

- if the "wave cycle" has only one wave, it is simply a single wave, so only one maximum and one minimum will be available. These will be taken and memorized as peaks of the wave;

[7] See section 5.3.1.1

- if the "wave cycle" has more than one wave, the code will search the maximum and the minimum values, then it will calculate their averages value and it will take them as peaks of the cycle.

As soon as the peaks will be known, it will be possible to calculate the fiber's microstrain vector amplitude making a difference between the average of the maximums and the average of the minimum ones.

Vectors from actuator output files.
Within the actuator output file are written time [s] , position [μm] and voltage [V] of the test. It is necessary to calculate the microstrains starting from the actuator real position.
Considering the definition of microstrain:.

$$\mu\epsilon = \frac{\Delta L \ [m]}{L_0 \ [m]} \cdot 10^6$$

Where ΔL is the length variation of the fiber , or in this case the displacement of the actuator (expressed in meter), and L is the effective length of the fiber between the gluing plates, which is measured with a caliber.
Dividing each actuator position value for the effective length, it is possible to obtain the "actuator microstrain vector".
At this point, the code will research the maximum and the minimum values, as before the number of the concatenated waves influences the procedure:

- if the "wave cycle" is composed by a single wave, the code will take the only and available value for maximum and minimum, setting them as peaks;

- if the "wave cycle" is composed by exactly 2 waves, the code will take the last maximum and minimum value to avoid transitory effect influence;

- if the "wave cycle" is composed by more than 2 waves, the code will search only the maximum and minimum values correspondant to the last waves of the wave cycle.
  In particular there will be taken in consideration only the waves in the

last quarter of the wave cycle, except for the last one[8]. After that it will calculate the averages of the maximum and the minimum values detected, and it will take them as peaks.

As soon as the peaks will be known, it will be possible to calculate the actuator's microstrain vector amplitude making a difference between the average of the maximums and the average of the minimums.
Taking a wave cycle composed by several waves, if the controller's memory allows it, will greatly reduce the effect of possible transitory effects.

Once that the amplitude of the fiber and of the actuator has been computated, it is possible to obtain their ratio, considering the actuator's microstrain vector as the input and the fiber's microstrain vector as the output.
The ratio, expressed in decibel, is then calculated as:

$$20 \cdot log_{10}\left(\frac{output}{input}\right) = 20 \cdot log_{10}\left(\frac{\mu\epsilon_{fiber}}{\mu\epsilon_{actuator}}\right) \tag{5.1}$$

This script's result is the amplitude ratio of a single frequence, as shown in figure 5.15; to obtain the complete analysis several tests at different frequencies must be done. The programm must be run for each desired frequency of the analysis, the results provided has to be saved in a Excel file.

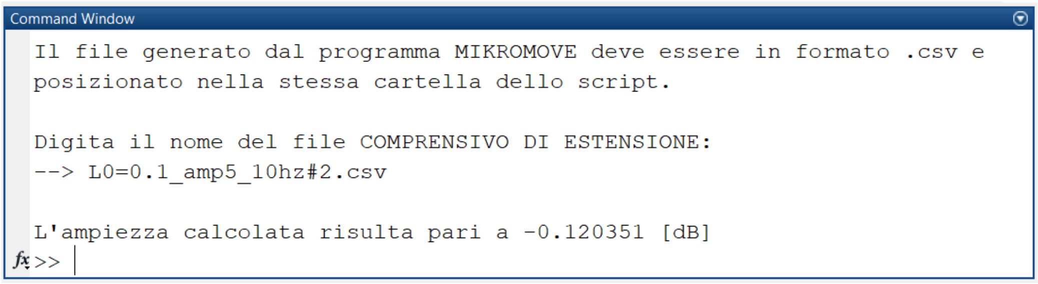

Figure 5.15: *Analisi_dinamica.m* result

[8] A numeric example makes easier the comprension: suppose that the user sets the maximum number of concatenated waves to 10. The code will search the maximum and the minimum values starting from the first wave of the last quarter to the penultimate wave of the wave cycle, so the code will search the values in the interval from ($0.75 \cdot 10 = 7.5 \rightarrow 7th$) the 7th to the 9th wave.

5.3.2 Diagrammi Bode sperimentali.m

This script can be run only after that all the measurements of the analysis have been done and saved into a precise Excel file. To save the analysis results provided by the preovius script, it is necessary to use the structure of the file Excel *Misure_schema_foglio*, figure 5.16, provided within the folder with all the MATLAB programms.
Here are summarized the instructions and the column features of this Excel file:

- *Frequency* is the column on which writing the frequencies used to make the analysis, no empty rows have to be left;
- *Commanded amplitude* is the column on which writing the desired displacement amplitude inserted in the wavegenerator tool;
- *Real amplitude* is the real amplitude reached by the actuator. This is effectively a dynamic system of second order so it surely will respond with some attenuation;
- *Theoretical amplitude* is the amplitude to which the user wants to make the analysis. It is clear that the real amplitude has to be the nearest possible to this value, if the real one is too attenuated, the command amplitude has to be modified in order to make real amplitude as near as possible to theoretical amplitude;
- *test*, in these columns is possible to load a maximum of four test results, each test has to be done with the same frequencies and at the same amplitudes;
- *Average value*, in this column the average value of the precedent test results is calculated. Making an analysis with more than one test helps to reduce randomly errors which can occur during the measurements.

This file has to be manually put in the same folder of *Diagrammi_Bode_sperimantali.m*, once all the numbers have been inserted within the table the script can be run.
The table structure is shown in figure 5.16.

	A	B	C	D	E	F	G	H	I
1									
2	Insert test specification: amplitude of the command, effective length of the fiber.				BODE FIBER				
3	FREQUENCY [Hz]	COMMANDED AMPLITUDE [μm]	REAL AMPLITUDE [μm]	THEORETICAL AMPLITUDE [μm]	TEST 1 [dB]	TEST 2 [dB]	TEST 3 [dB]	TEST 4 [dB]	AVERAGE VALUE [dB]
4	5								
5	10								
6	20								
7	25								
8	50								
9	75								
10	100								
11	150								
12	200								
13	250								
14	300								

Figure 5.16: *Misure_schema_foglio* Excel file structure

As visible in figure 5.17, the MATLAB program will request the name of the folder on which the user desires to save the figures produced. Then, the script will request the name of the file Excel on which all the analysis data are available.

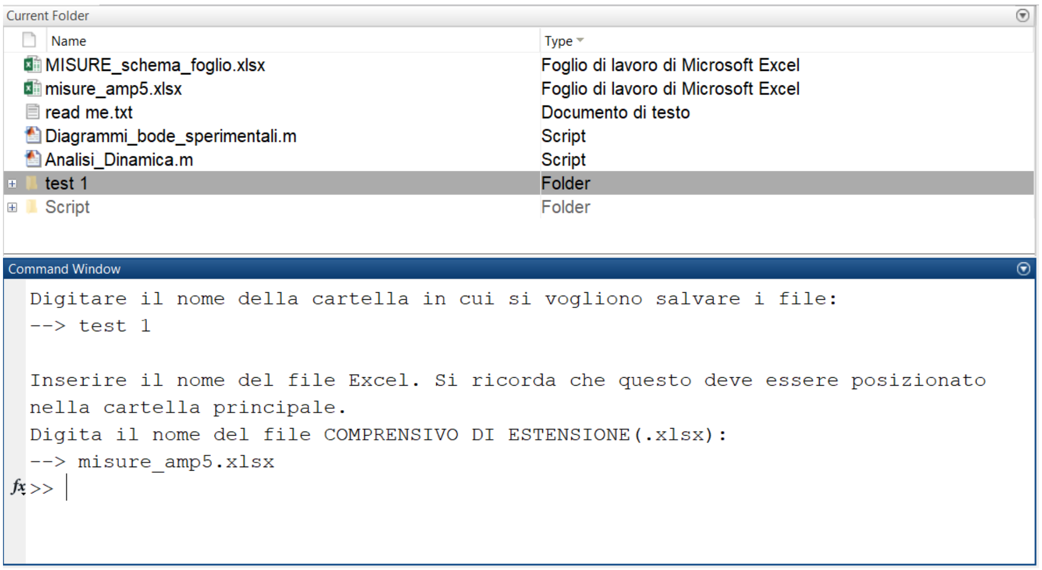

Figure 5.17: *Diagrammi_Bode_sperimantali.m* command window

The script will automatically produce and save the Bode diagram of each test, the Bode diagram of the test's average value and the Bode diagram of the actuator. These graphics will be saved in format *.png* and as *MATLAB figure* in the created folder, as visible in figure 5.18.

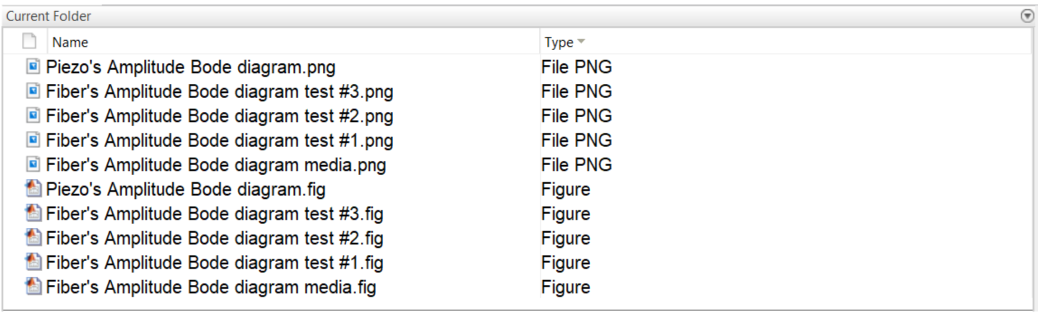

Figure 5.18: Graphics generated by the script

An example of the Bode diagrams generated by the script is in figure 5.19, in this case the actuator's and the test's average value graph are shown. In order to obtain a graph with a tendency line, a "Least square" approximation of the data has been done.

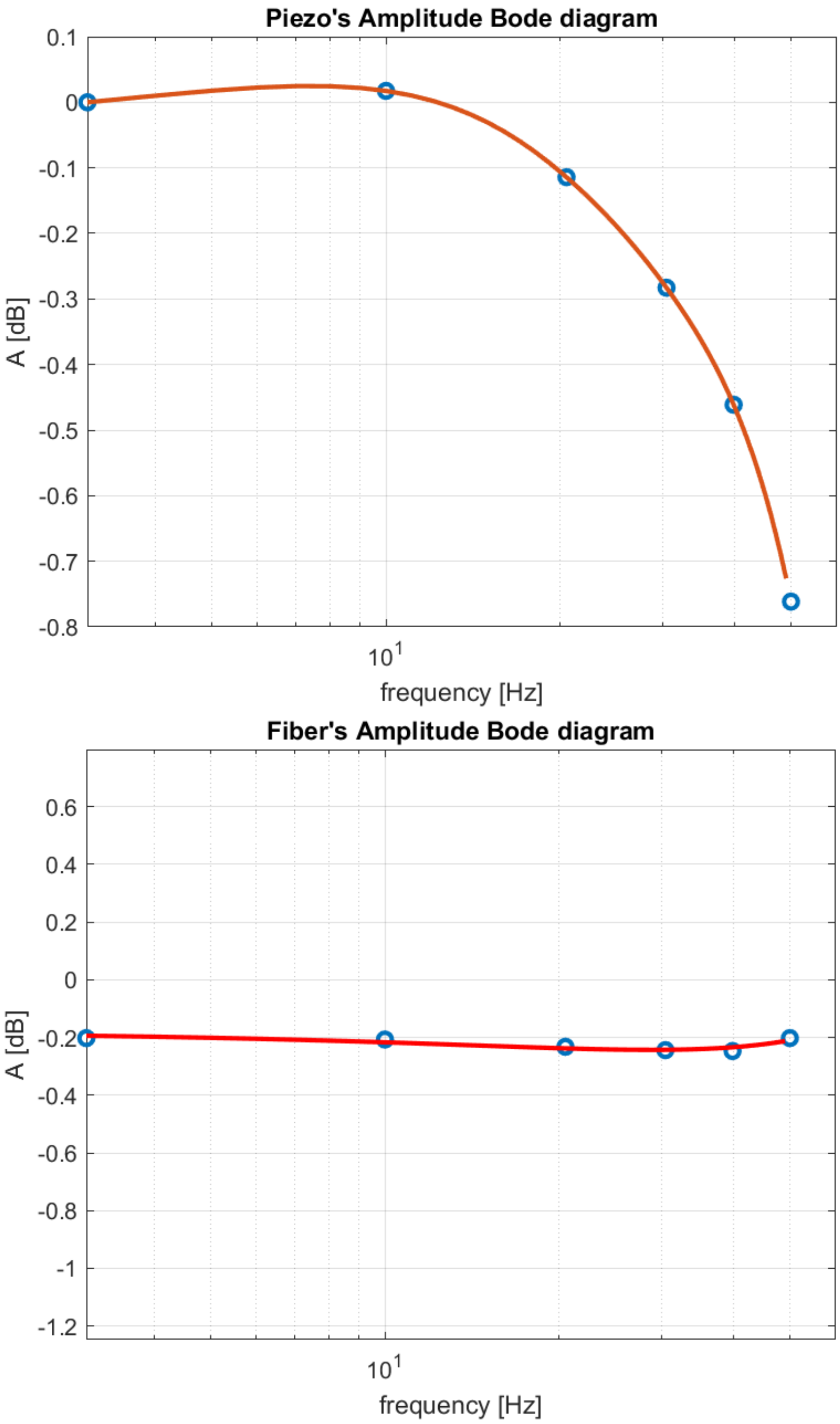

Figure 5.19: Example of actuator and test's average value Bode diagram

Chapter 6

Tests and Observations

In this chapter will be reported the results of the tests, using Bode diagrams, and the relative observations. It will describe the fiber's behaviour at low and high frequency, studying how factors, such as pretension or command's amplitude, may influence the measurements.

6.1 Low Frequency Tests

In this section is analyzed the behaviour of the fiber subjected to sinusoidal commands at low frequency, in particular it focus on the repeatability of the tests and the influence of factors, such as command's amplitude and the fiber's pre tension, on the measurement.
The repeatability has been analyzed comparing several tests' results to which the same input has been given, the influence of the command's amplitude has been studied looking at the the fiber's behaviour differences providing different amplitude inputs.

6.1.1 Test 1, Repeatability effect

This test purpose is to analyze the repeatability of the measurements.
Figure 6.1 shows the results of tests made with an amplitude of 5 μm and an effective length of 0.1 m.
Comparing the different tests at the same amplitude, some variations of the entity of $\approx$ 0.1 dB are present.

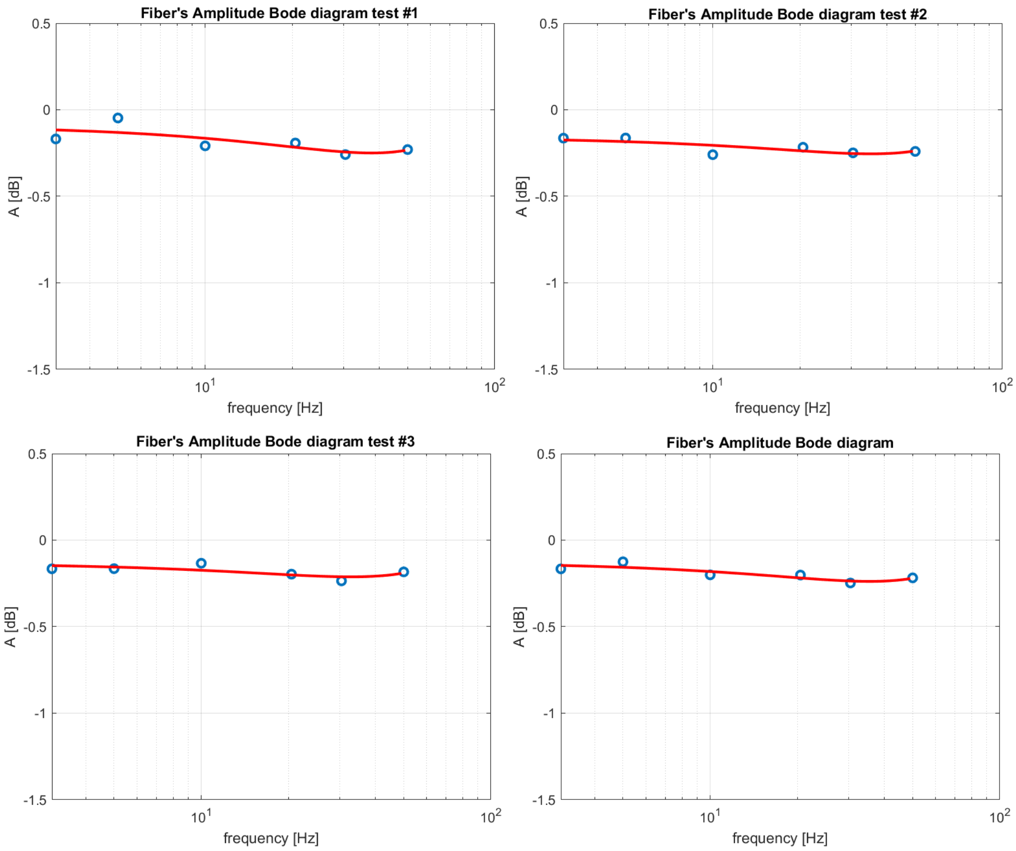

Figure 6.1: Tests and mean measure with amplitude 5 μm and effective length 0.1 m

The reasons of these variations are the fluctuations on the fiber's microstrains values due to the sensitivity of the interrogator. The *SmartScan SBI* is able to provide a measure with an error of $\pm$ 0.0008 nm that, translated in microstrain, is $\approx \pm$ 0.65 $\mu\epsilon$.
Let's consider now the measurements provided by the interrogator and converted from wavelength to microstrain, figure 6.2 shows the microstrains variations at frequency of 5 Hz of two different tests, in particular the test #1 and the #3.
Looking at the time interval between 0 and the tests' starting points, a difference is evident: the test #1 shows a relevant number of peaks while the test #3 just few. This proves the random nature of the fluctuations phenomenon, which can affect the whole measurements in any time value and

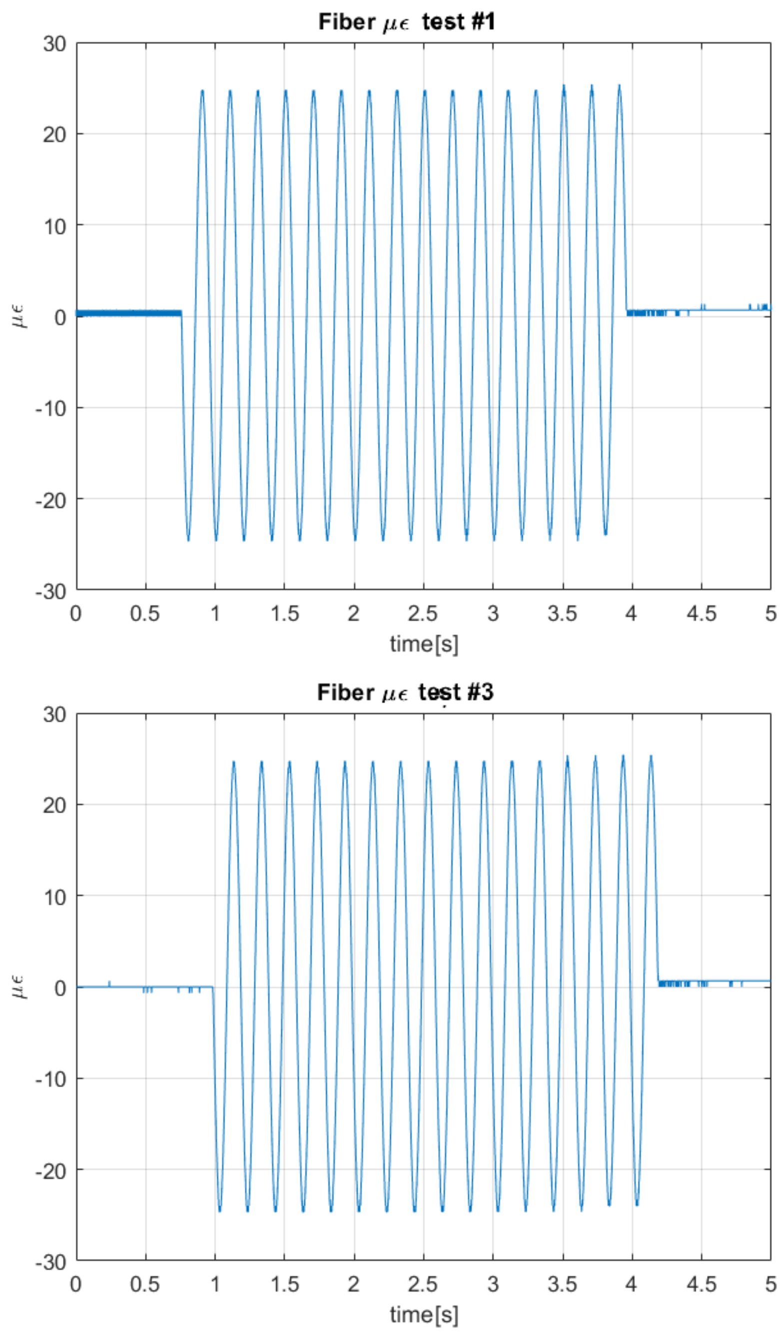

Figure 6.2: $\mu\epsilon$ variations for test 1 and 3 at a frequency of 5 Hz. Command's amplitude 5 μm and effective length 0.1 m

for a not defined number of times.
What has just been said means that every value may be influenced by these peaks, not only the values read when the fiber is motionless, so also the maximums and the minimums may be "dirtied", affecting the fiber's singal amplitude calculation.
In this tests' condition, with an effective length of 0.1 m and an amplitude of the commanded signal of 5 μm, the fluctuations influnce is not so relevant, they will produce a small variation of the $\mu\epsilon$ amplitude values. A variation of 0.65 $\mu\epsilon$ on an amplitude of $\approx$ 50 $\mu\epsilon$ is almost negligible.
If the amplitude of the command is increased, for example to 10 μm, also the amplitude of the microstrains variations will increase, making the fluctuations less and less important, as shown in figure 6.3.

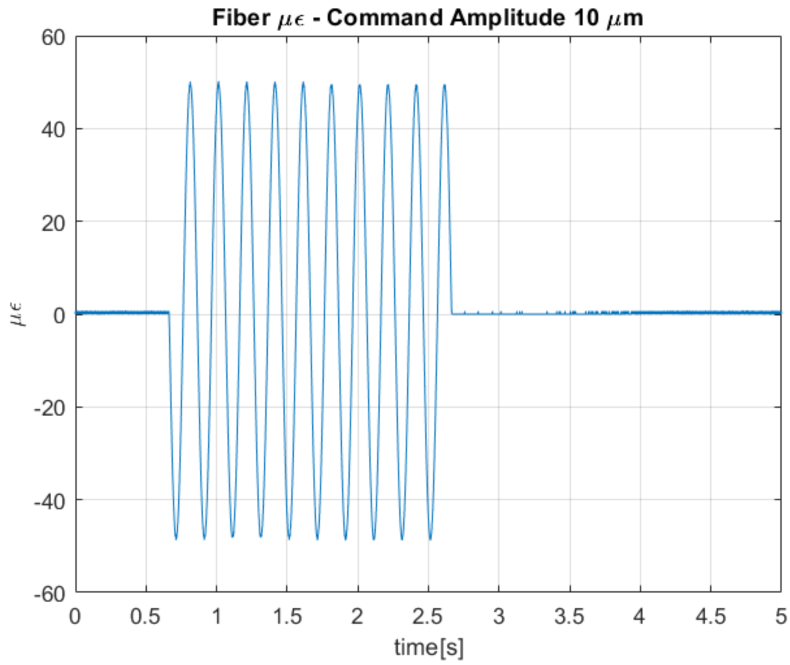

Figure 6.3: $\mu\epsilon$ at a frequency of 5Hz. Command's amplitude 10 μm and effective length 0.1 m

With a microstrains' amplitude of $\approx$ 100 $\mu\epsilon$, the impact of the $\pm$ 0.65 $\mu\epsilon$ fluctuation will be attenuated and the points on the Bode diagrams will be distrubuted more homogeneously, as visible in figure 6.3.

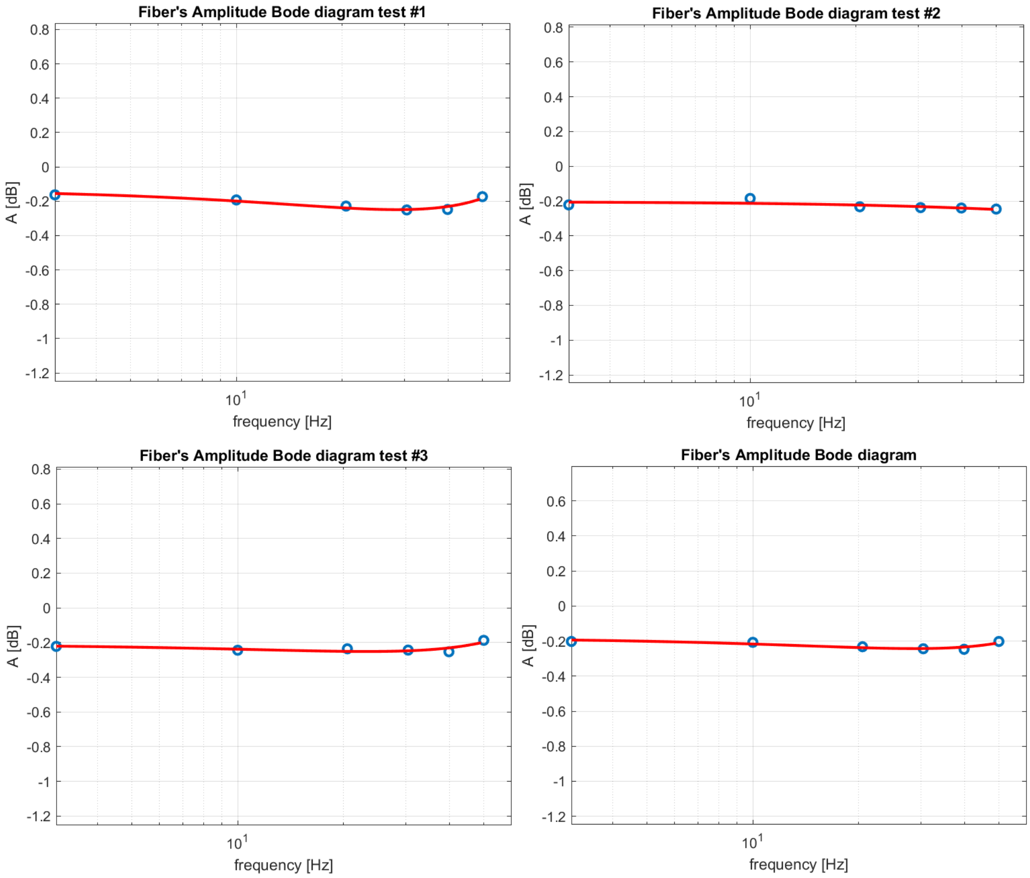

Figure 6.4: Tests and mean measure with amplitude 10 μm and effective length 0.1 m

Until now, tests have been done with a fiber's effective length of 0.1 m and displacement of some micrometers, but what happen if the effective length of the fiber is increased significatively or the displacement of the actuator is reduced? The answer to this question is in the definition of *microstrain*. Reminding that:

$$\mu\epsilon = \frac{\Delta L}{L_0}$$

with L_0 effective length of the fiber and ΔL the displacement of the actuator. It appears clear that if the length is increased the value of the $\mu\epsilon$ of both the actuator and the fiber will decrease significatively.

When the fiber's effective length is increased so much (or the command amplitude is decrased so much) that the fiber's microstrains amplitude is comparable with the sensitivity of the interrogator, the reliability of the measure is compromised, and so the repeatablity of the different tests.
The reason is simple, as said previsusly the fluctuations have a random nature, so they can affect the measurement on the maximums and on the minimums a non definite number of times. In addition to this the $\pm 0.65\ \mu\epsilon$ variations heavily incide on the fiber $\mu\epsilon$ amplitude and, considering that the piezoactuator $\mu\epsilon$ amplitude is constant, on the Bode values computated[1].
Showing the experimental results will clear what have previously said.

In order to prove what previously said, these last tests have been done using a new fiber with an effective length of L0 = 0.45 m.
The amplitude computated are shown in figure 6.5 as visible 4 tests have been done for each frequency.

L0=0,45 m Ampiezza 2 FOGLIO RIASSUNTIVO				BODE AMPLITUDE [dB]			
FREQUENCY (Hz)	COMMANDED AMPLITUDE (µm)	REAL AMPLITUDE (µm)	THEORETICAL AMPLITUDE (µm)	TEST 1	TEST 2	TEST 3	TEST 4
PROVA A 1000 µε- PRETENSIONAMENTO STANDARD							
5	2	2	2	0,3185	1,5184	0,3176	0,3164
10	2	2	2	0,7225	0,7203	1,0251	0,6208
25	2	2	2	0,6164	0,4552	0,4540	1,2395
50	2,3	3	2	1,2357	0,3231	0,9947	0,1698
100	3	1,98	2	0,3006	0,5960	1,0842	0,4606

Figure 6.5: Tests and mean measure with amplitude 2 μm and effective length 0.45 m

Tests 1,2,3 and 4 have been made in sequence for each frequency. The results have no scientific valence, they haven't a tendency when the frequency is increased and the repeatability is compromised beacause of the great values differences between tests at the same frequency.
Looking at the result of tests #1 and #2 at 5 Hz this appears really clear, an increase of 1.2 dB makes no scientific sense , figure 6.6 shows the reasons.

[1]Remember that the Bode values are computated as $20 \cdot log_{10}\left(\frac{\mu\epsilon_{fiber}}{\mu\epsilon_{actuator}}\right)$

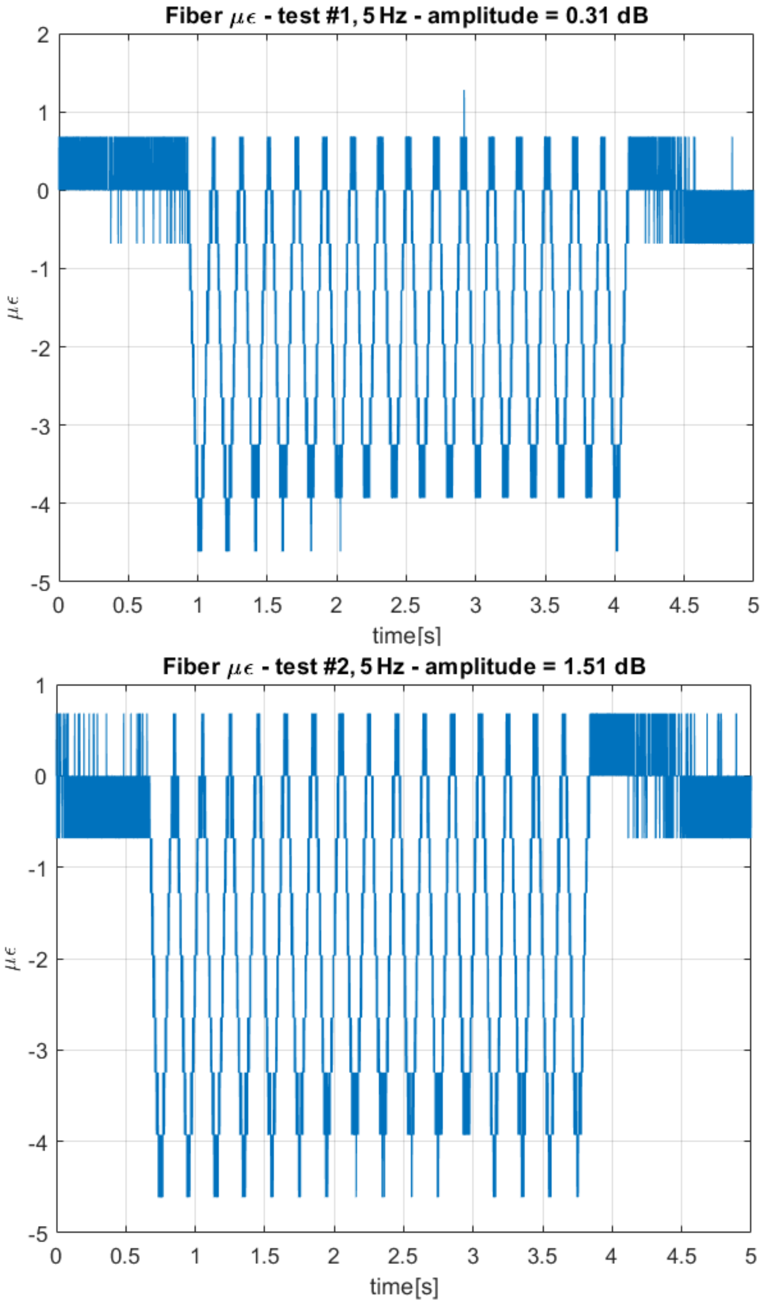

Figure 6.6: Tests #1 and #2, 5 Hz, amplitude 2 μm and effective length 0.45 m

The difference of amplitude due to the fluctuation peaks is about 1.2 $\mu\epsilon$ in some time values, moreover, the number of peaks present on the maximums and the minimums values of the test #2 is definitely greater respect to the number of the test #1. This affects the mean value of the amplitude that, rapported to the constant actuator's amplitude, produce a greater Bode's diagram value.
The influence of the fluctuations peaks is now really important, since that the maximum amplitude of the fiber of the tests in figure 6.6 is ≈ 5 $\mu\epsilon$.

Observations and conclusions
In order to guarantee a measurement with scientific valence and the repeatability of the tests, the amplitudes of the fiber's microstrains must be at least 20 - 25 $\mu\epsilon$, below this value the results produced are meaningless.
The amplitude restriction has consequences for the effective length of the fiber, which is in turn limitated by the maximum displacement of the piezoelctric actuator and the attenuation of the piezoactuator system.
For example, it is possible to obtain ≈ 30 $\mu\epsilon$ fiber's microstrains of amplitude with a displacement of the piezoactuator of 30 μm, value near the maximum available, and an effective length of 1 m, but only at very low frequence. At higher frequency, over 25 Hz, the actuator starts to attenuate and it is necessary to select an higher command amplitude to provide the same real input of 30 μm, which is not available.
However, it would be better to avoid working near the maximum actuator's displacement values, in order to preserve its life.
The correct values to obtain results with scientific meaning are:

- effective length, $L_0 < 0.4$ m;
- actuator's command amplitude, 2 - 20 μm.

These two factors are proportional, small command's amplitudes suit for small effective lengths, large command amplitudes for great values of effective length.
Under these condition it is then not necessary to repeat several times the same test for each frequency and mediate the values, but it possible to take the measure with a single test per frequency.

6.1.2 Test 2, Amplitude effect

The fiber's mean measure of the previously tests, amplitude 5 μm and 10 μm, have been chosen to analyze the influence of the amplitude on the measurements.
Figures 6.7 and 6.8 show the behaviour of the fiber. As visible, despite the fact that the amplitude is varied, the values and the trend line are the same, except from really small differences.
It can be concluded that the amplitude doesn't affect the results of the measurement.

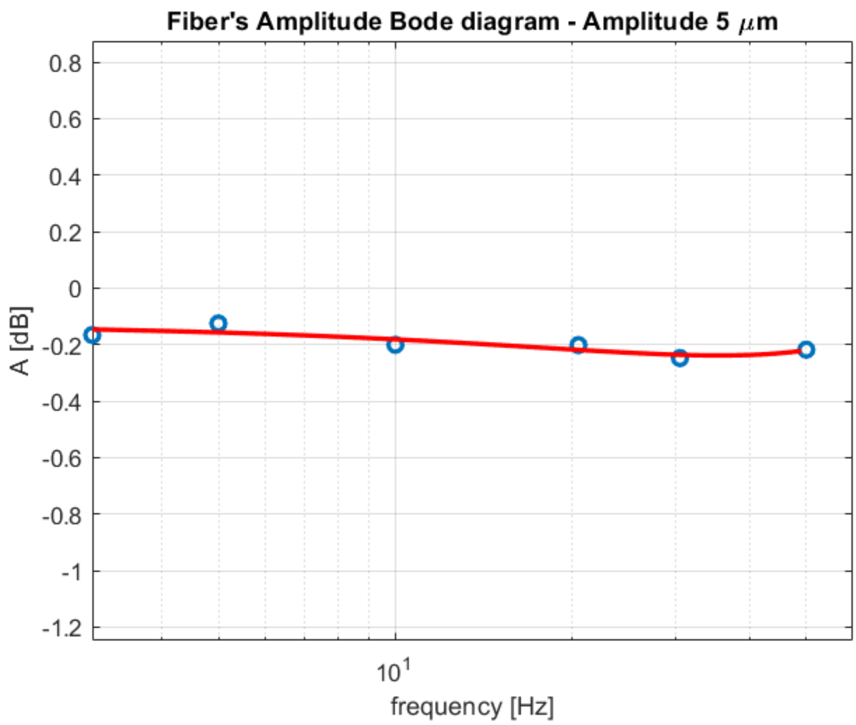

Figure 6.7: Low frequency test, mean measure of a commanded amplitude of 5 μm, effective length 0.1 m

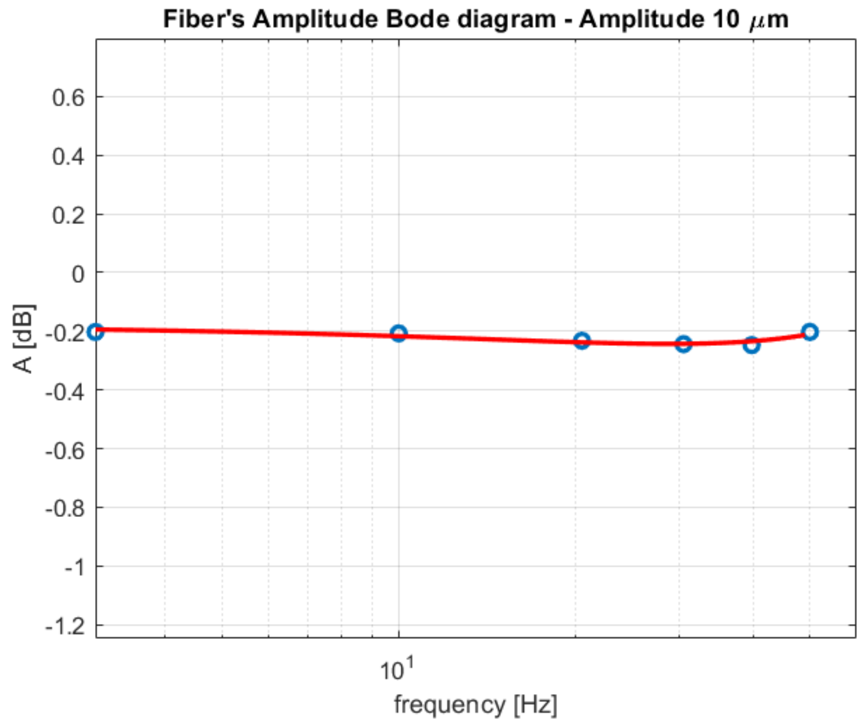

Figure 6.8: Low frequency test, mean meausure of a commanded amplitude of 10 μm, effective length 0.1 m

6.1.3 Test 3, Pretension effect

Two tests with a command amplitude of 5 μm and different pretensions have been made. The first one has been executed with a pretension of 1000 $\mu\epsilon$ while the second test has been executed applying 2000 $\mu\epsilon$. The tension on the fiber has been selected rotating the micropositioner in order to pull the fiber, the exact value of the strain has been read by means of the Smartscan software, selecting "enhanced acquisition" and setting the FBG as a strain sensor. Figure 6.9 shows the results of the two measurements, the tests has almost the same values and tendency line, which is $\approx$ - 0.2 dB.
It can be concluded that, in the order of these pretension values, the fiber's behaviour is not affected by the pretension applyied, however the explanation of this phenomenon is not as simple as it seems, so a more detailed description will be given in the subsection 7.2.3.

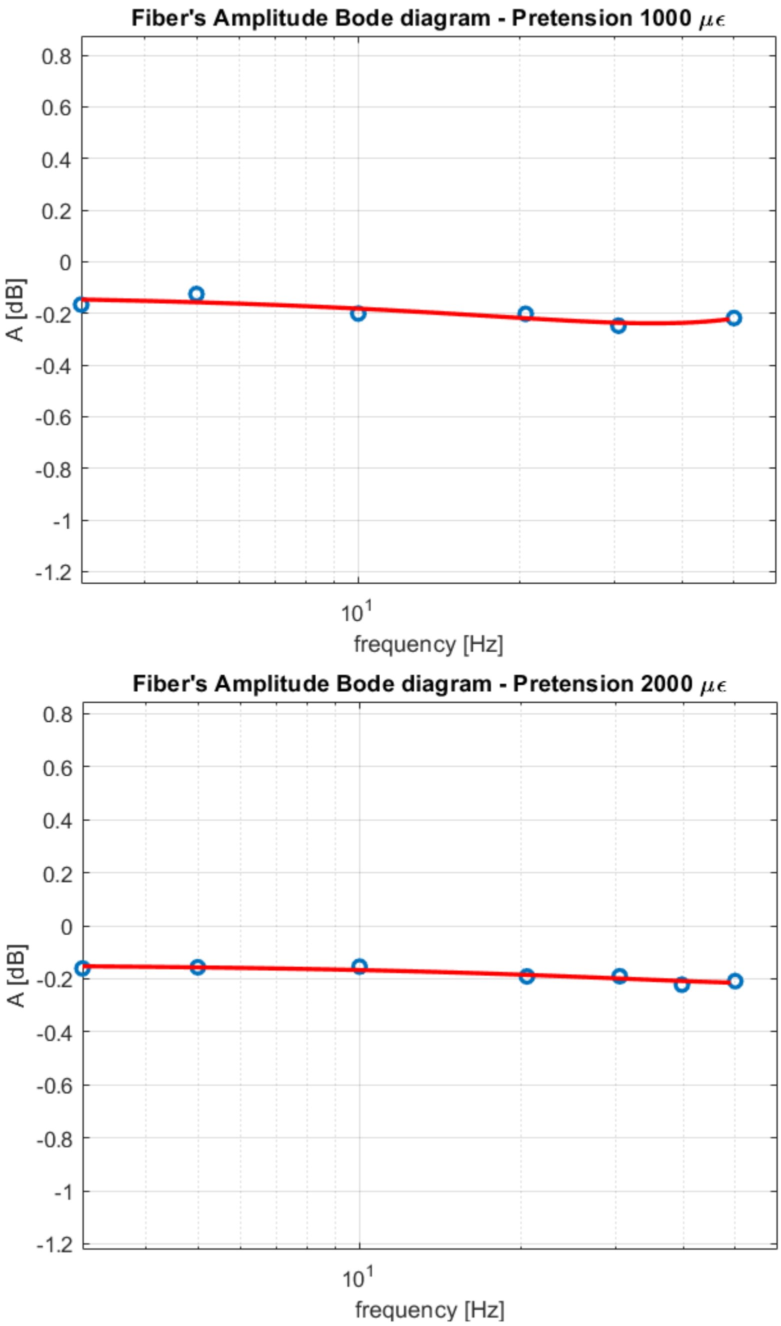

Figure 6.9: Low frequency tests, mean meausure, amplitude of 5 μm, pretension of 1000 $\mu\epsilon$ and 2000 $\mu\epsilon$, effective length 0.1 m

6.2 High Frequency Tests

In this section, tests with a maximum frequency of 250-300 Hz have been conducted, all the effects described in sections 6.1.1 and 6.1.2 are also considered valid for this type of analysis while what said in section 6.1.3 will be studied more in detail.
Before starting to study the pretension effect on the high frequency tests, it will be shown, in figure 6.10, a complete measurements, comprehensive of low and high frequency values.

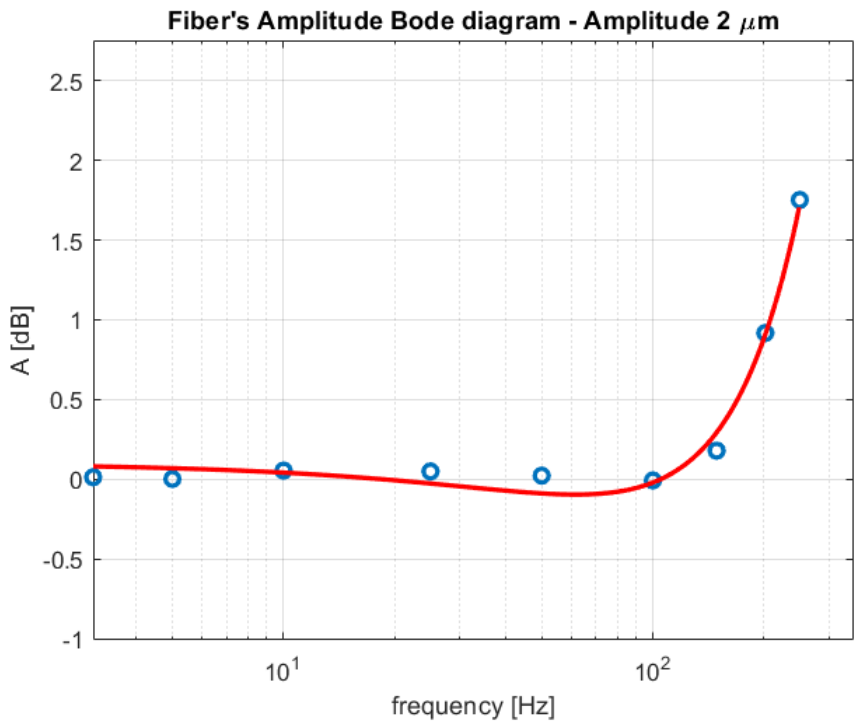

Figure 6.10: Test at high frequency, amplitude 2 μm, effective length 0.1 m

As visible, until the frequency of 100 Hz, the fiber's behaviour is the same of the low frequency tests. Over this frequency, the fiber starts to amplify the input to which is subjected.
This result has been completely unexpected, two possible causes of this behaviour may be the influence of the fiber's natural frequency on the test, or the incorrect values provided by the *PIMikroMove* software. It is then nec-

essary find a way to estimate the natural frequency of the system (studying if and how it influence the measure) and a way to verify the data provided by the software; both will be better analyzed in chapter 7.
With a frequency range wider respect to the one used in the low frequency tests, it is possible to obtain a more detailed Bode diagram of the piezo actuator, shown in figure 6.11.

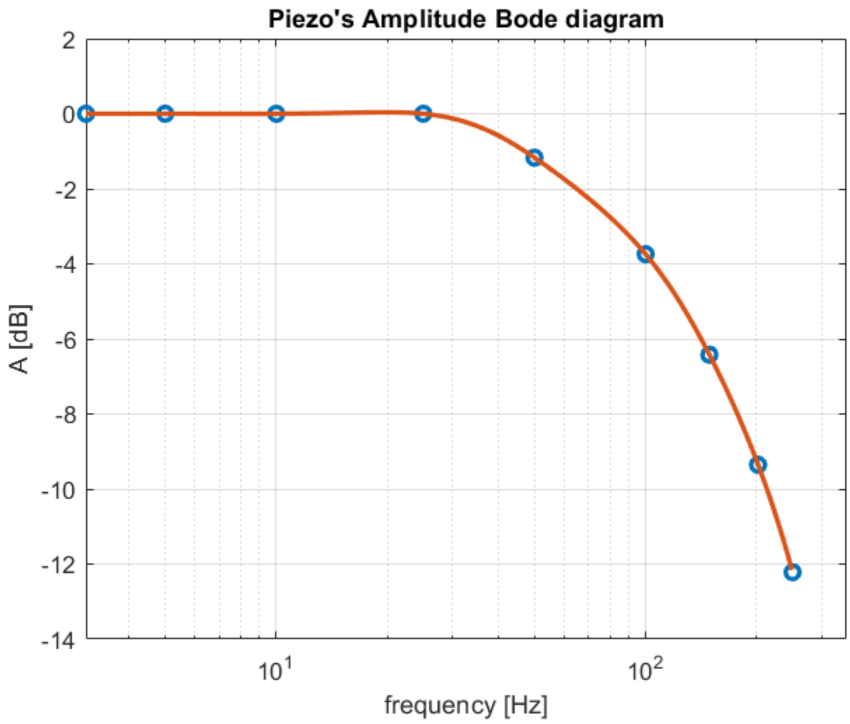

Figure 6.11: Piezoelectric actuator's Bode diagram

The actuator's Bode diagram shows a constant value of 0 dB when it moves with low frequency, this means that the system respond exactly with the commanded amplitude. At high frequency it presents high values of attenuation, such as -12 dB at 250 Hz, which limit heavily its use with frequencies above 250-300 Hz.

6.2.1 Test 4, High frequency - Pretension effect

Three tests with command amplitude 2 μm, effective length 0.1 m and different pretension have been conducted: the first one has been made with 500 $\mu\epsilon$, the second with the "standard" pretension of 1000 $\mu\epsilon$ and the last one with 2000 $\mu\epsilon$, figure 6.12 shows the results of the measurements.

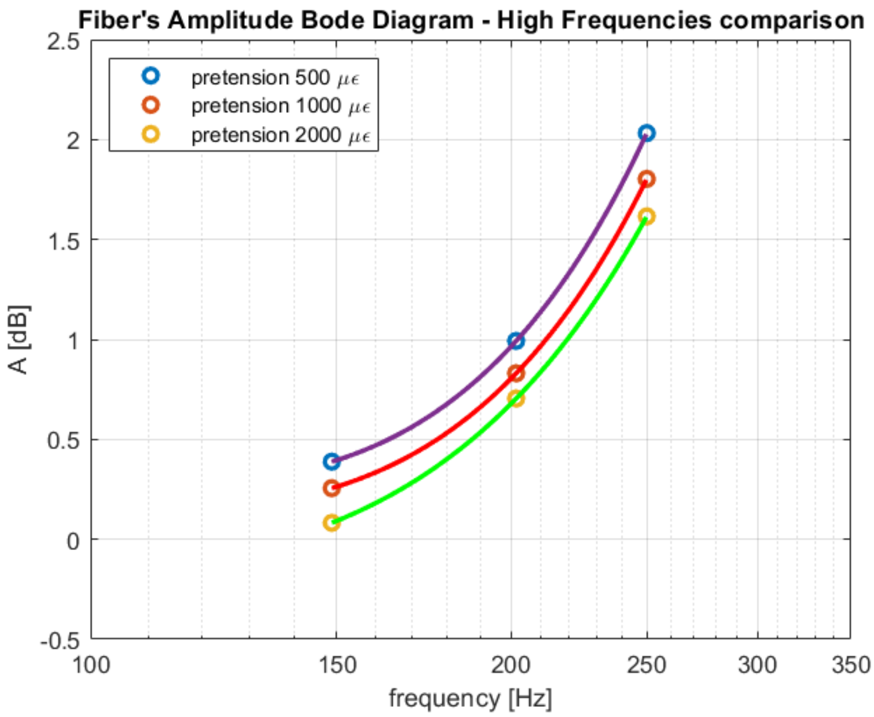

Figure 6.12: High frequency tests comparison, amplitude 2 μm, effective length 0.1 m

The high frequency tests show a dependency from the pretension of the fiber, the more the pretension is increased more the amplification is shifted to lower values. As said in section 6.1.3, the causes of the fiber's behaviour under the pretension effect will be better explained in chapter subsection 7.2.3.

Chapter 7

Arduino Measurement System & Fiber's Natural Frequency Influence on Tests

In this chapter will be investigated the values' correctness of the piezoelectric actuator, provided by the software PIMikroMove, and the influence of the natural frequency of the fiber on the measurements.
To validate the actuar's values, external devices have been used , in order to have a second source of values which can be compared to the software ones. The influence of the natural frequency is evalueted both sperimentally and using the standing waves theory.

7.1 Arduino Measurements System

Before describe the Arduino setup used for the measurements, it is necessary punctualize which values of the software will be releved and compared.
The actuator's frequency will be the object of interest, other values, as its real position, won't be. The objective is the validation of the frequency to which the actuator is moving, this will be done comparing the value of frequency imposed by the user, in the "Wave Generator Tool", with the effective frequency releved by an external sensor.
The choice of the external sensor has been made considering that it must provide a time evaluation of a physic quantity, in order to obtain the motion

frequency. The nature or the value of the physic quantity measured is not vinculating. An accelerometer has been chosen as external sensor, this, once fixed to the actuator, will provide the acceleration values to which it is subjected.
The accelerometer must be powered to produce and save the measurements' values, the easiest way to do it is using an Arduino interface, in particular "Arduino uno" has been chosen.
The simpliest "sensor to PC" configuration should be *sensor* → *Arduino* → *PC*, using the serial protocol (SPI) to communicate. However, the direct communication is too slow to register and write on a file all the data measured by the accelerometer, in this way a lot of values would be lost.
It is then used a memory support, with a high file's writing speed, on which write the data measured by the accelerometer. When the measure will terminate, it will be possible to access the file inserting the memory on the PC. Figure 7.1 shows the logic of the arduino system, an Arduino microSD shield has been used to store the data.

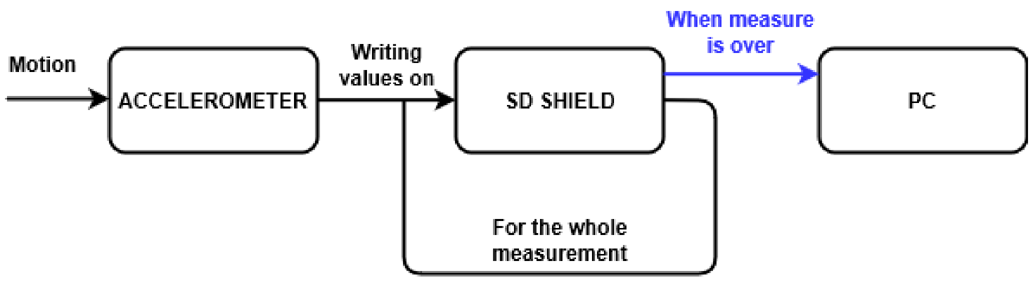

Figure 7.1: Arduino system flowchart

Accelerometer - ADXL 345

The *ANALOGIC DEVICE - ADXL 345* is the accelerometer used to measure the acceleration values of the commanded motion. It has a maximum sample rate of 3200 Hz and a maximum measurement range of ± 16 g, both are selectable by the user on a list of avaliable values which the producer provide. All the sensor information are available in the *ADXL 345 datasheet* [19].

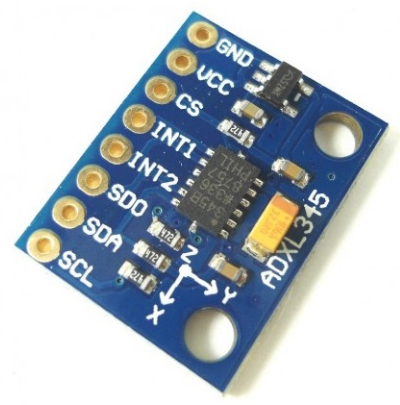

Figure 7.2: Analogic Device - ADXL 345

MicroSD shield

This is the module on which insert the microSD card in order to save the data measured by the sensor. It is simply mounted over the "Arduino uno" and it allows to connect external devices by means of the same pins of the Arduino, which are replicated on the shield. The sensor is in fact linked to the shield's pins.

Figure 7.3: MicroSD shield

Wiring Diagram

Figure 7.4 shows the electring wiring between the accelerometer, the SD shield and Arduino UNO. The shield is installed on the Arduino UNO and the sensor is wired to the SD shield using I^2C communication interface. The sensor needs to be wired with the Ground, GND, the power pin, $5V$, the data line, SDA and the clock line, SCL.

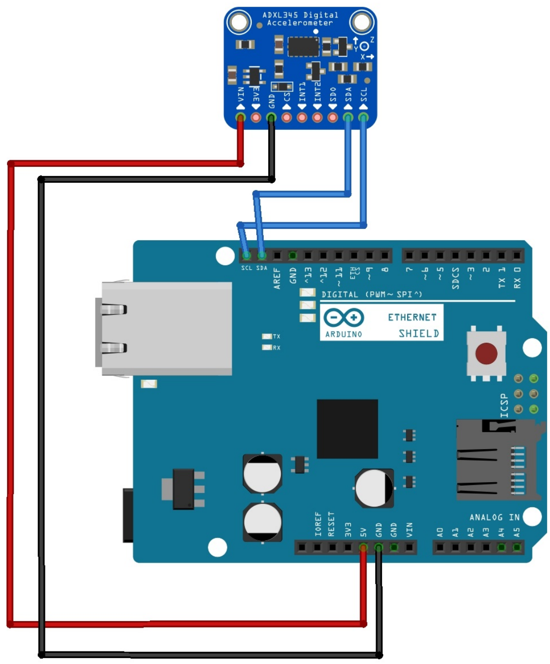

Figure 7.4: Arduino wiring diagram

Codes

Looking now at the software side, it has been necessary to put all the functions of the single devices together. Two codes have been developed: the first one commands the Arduino, in order to write the accleration values on a text file (which is stored on the microSD card), the second one is a MATLAB script which evaluates, interpoles and plots the results.

Arduino code: it starts the serial communication, checks if a microSD is inserted on the shield and if a text file named "TEST" is already present on the memory. If the file already exists, the code will elimanate it and it will create a new one. Once entered in the command window, the user must press s to start the measurement and a to finish it.

In order to maximaze the writing speed on the SD card, only the time and the X axis' values are written on the text file, the Y and the Z values are not of interest. For the same reason, considering that the writing speed is $\approx$ constant, only a value of time every twenty is written.
In this way, it has been possible to obtain a writing speed of 0.0022 seconds, and so a sampling frquency of $\approx$ 454,5 Hz. This means that, according to Nyquist theorem, is possible to measure tests until 45.5 Hz or little more (50Hz).

MATLAB script: once imported the "TEST.TXT" file's values with the MATLAB function "import data"[1], it interpoles the time's column empty cells and it provides a graph with the measurements of the sensor in function of the time.

Complete setup

The accelerometer has to be fixed to the actuator in order to read the measure of its movement, at this purpose a support plate has been designed and 3D printed.

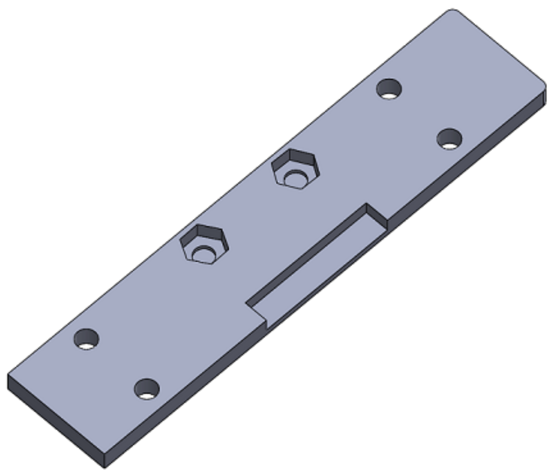

Figure 7.5: Solidworks accelerometer support plate design

The four through holes allows the support plate to be fixed to the actuator,

[1]It is necessary to import the data as a numeric matrix for the correct working of the script

two exagonal seats of the dimension of M2.5 nuts have been obtained, the nuts have been inserted in these, allowing in this way to fix the accelerometer to the support plate. The complete setup is shown in figure 7.6.

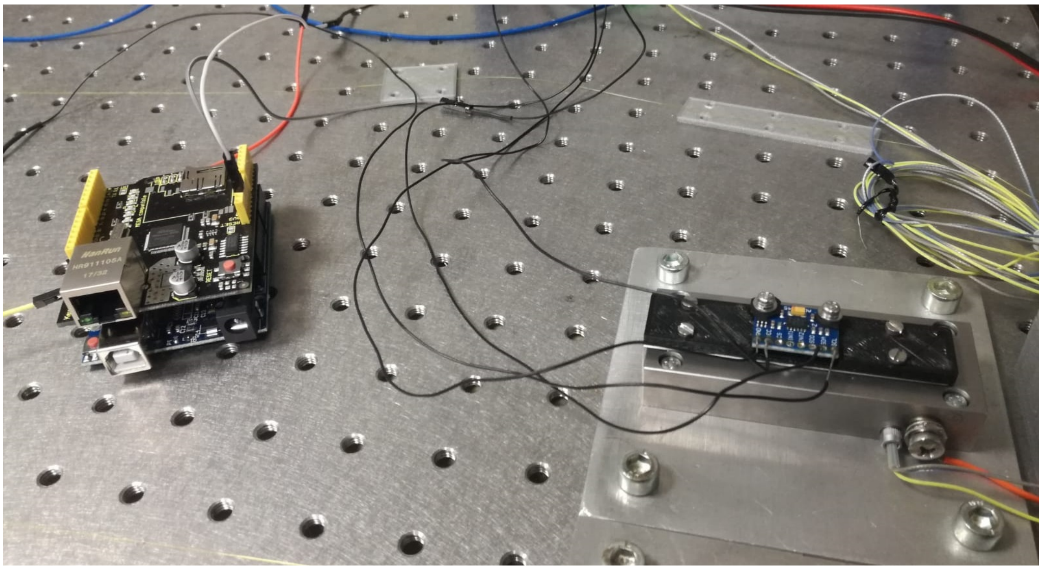

Figure 7.6: Arduino measurement system complete setup

Results

Several tests at low frequency and small amplitude have been done, but the noise produced by the sensor compromise the measurements, under these conditions is not possible to devide the noise from the measurements values. In order to avoid this influence, measurements near the maximum frequency measurable and with a command's amplitude near the maximum displacement have been made.

Two tests with a constant amplitude of 35 μm and different frequency have been conducted, figure 7.7 shows the results.

In the central part of both the tests, where the peaks are higher, is where the actuator were in motion, before and after this interval, the tests is characterized by sensor's noise.

The frequency of the test have been calculated choosing manually two peaks in sequence and looking their time values, the difference between these values is the period of the sinewave.

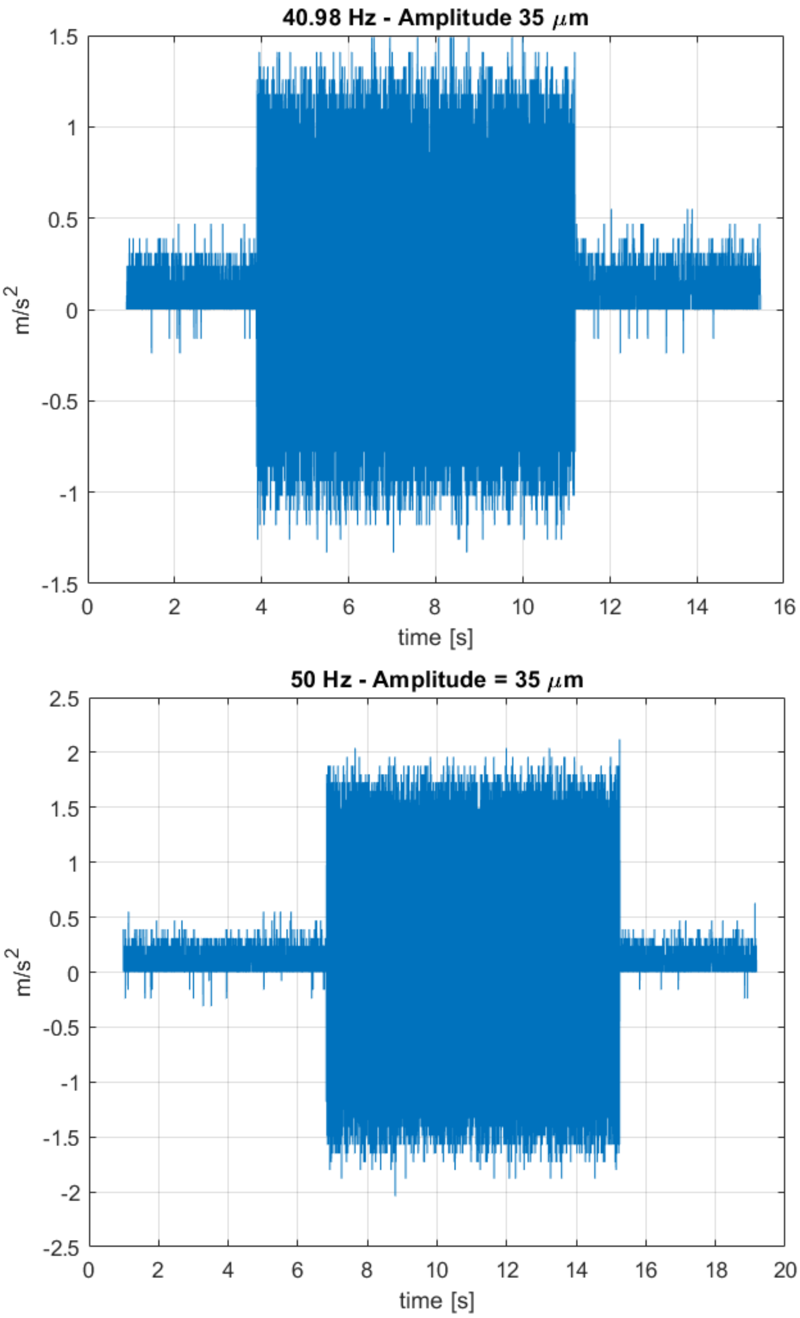

Figure 7.7: Tests at 40.98 Hz and 50 Hz, amplitude 35 μm

By $f = \frac{1}{T} = \frac{1}{t_2 - t_1}$ the frequence has been calculated. To validate the measure several couples of peaks, chosen in random way, have been taken. All of these, once computed, has shown freqeuncy values very close to the commanded ones, the first test's calculated values were ≈ 39.8 Hz while in the second test's frequencies were ≈ 51 Hz.
It can be said that the values provided by the PIMikroMove software are correct, the small values' differences are imprecisions of the whole Arduino measurement system.

7.2 Fiber Optic's Natural Frequency Influence on the Tests

Having validate the values provided by the PI software, it remains to study the influence of the natural frequency on the measurements.
An explanation to the results of figure 6.10 may be researched in the test bench's setup and in the fiber's natural frequency. The setup used, shown in figure 4.11, constrains the optical fiber at the extremities, making it works as a vibrating string. At the sime time, it must be considered that every system, when subjected to a sinewave command with a frequency near its natural frequency, starts to amplificate the input value.
In order to prove that the fiber actually acts as a vibrating string, it must respect the *Standing Waves Theory.* The theory provide a formulation which allows to estimate the natural frequency of the string, if this value will be comparable with the one experimentally estimated it can be said that the fiber really acts as a vibrating string.
If this hypotesis is demonstrated, it will be analyzed how the natural frequency influence the tests.

7.2.1 Natural Frequrency Experimentally Estimate

It is possible to consider the fiber in the test bench setup as a guitar string. If the string is pinched, it will start to oscillate at its own frequency.
The fiber's own frequency can be determinated by pincing it and register its oscillations with the interrogator. Once that the measurement is registered, analyzing the time interval between two maximum or two minimum, it will

be possible to estimate the natural frequency of the fiber, according to:

$$f = \frac{1}{T} \tag{7.1}$$

It is very important to take again into account the Nyquist theorem, the sample rate of the interrogator must be setted at a value at least 10 times greater than the natural frequence, otherwise aliasing may occur. Obviusly the natural frequency is unknown so the maximum sample rate has been setted.

7.2.2 Standing Waves Theory & Theoretical Natural Frequency Calculation

The standing waves theory provide informations on the natural frequency and the relative armonics of a vibrating string.
The natural frequency of the string is called $fundamental$ while the harmonics are multiple of the natural one.
The result of the standing waves theory is the equation which provide the natural frequency, analytical demonstration is not of interest:

$$f = \frac{1}{2L}\sqrt{\frac{T}{\rho}} \tag{7.2}$$

Where:

- L is the effective length of the string;
- T is the tension to which the string is subjected;
- ρ is the linear density of the string.

The components T and ρ are not measurable directly but they can be calculated.

T values calculation

It is possible to compute the fiber's tension values considering the following formulation, derived from the Hooke's law [20]:

$$T = E_G A \frac{\Delta L}{L_0} = E_G A \epsilon \tag{7.3}$$

Where:

- E_G is the Young modulus of the fiber;
- A is the section's area of the fiber;
- ϵ are the strains to which the fiber is subjected.

The Young modulus term changes in function of the fiber's materials composition, a value of $\approx$ 20 GPa has been found in literature, [20], as value for fibers with polymide made coating.

The area is calculated simply with the circle's area formula, the diameter of the used fiber is $\phi = 155\ \mu m$.

The ϵ value is the microstrains value imposed with the micropositioner and divided by a factor of 10^6.

In table 7.1 are listed these values and three tension values at 500, 1000 and 2000 $\mu\epsilon$:

ϕ $[\mu m]$	A $[m^2]$	E_G $[GPa]$	ϵ	T $[N]$
155	$1.887 \cdot 10^{-8}$	20	$500 \cdot 10^{-6}$	0.1887
			$1000 \cdot 10^{-6}$	0.3774
			$2000 \cdot 10^{-6}$	0.7548

Table 7.1: Values and tension calculated at 500, 1000 and 2000 $\mu\epsilon$

ρ value calculation

No fiber's linear mass data are available in literature, so ρ has been experimentally computed, at this purpose a third fiber with effective length of 0.127 m has been used.

It has been experimentally estimated the natural frequency of this third fiber and then the value of ρ has been computed according to:

$$\rho = \frac{1}{4L^2} \frac{T}{f^2} \tag{7.4}$$

A test with 1000 $\mu\epsilon$ of pretension and $L_0 = 0.127$ m has been made, figure 7.5 shows the results of the test.

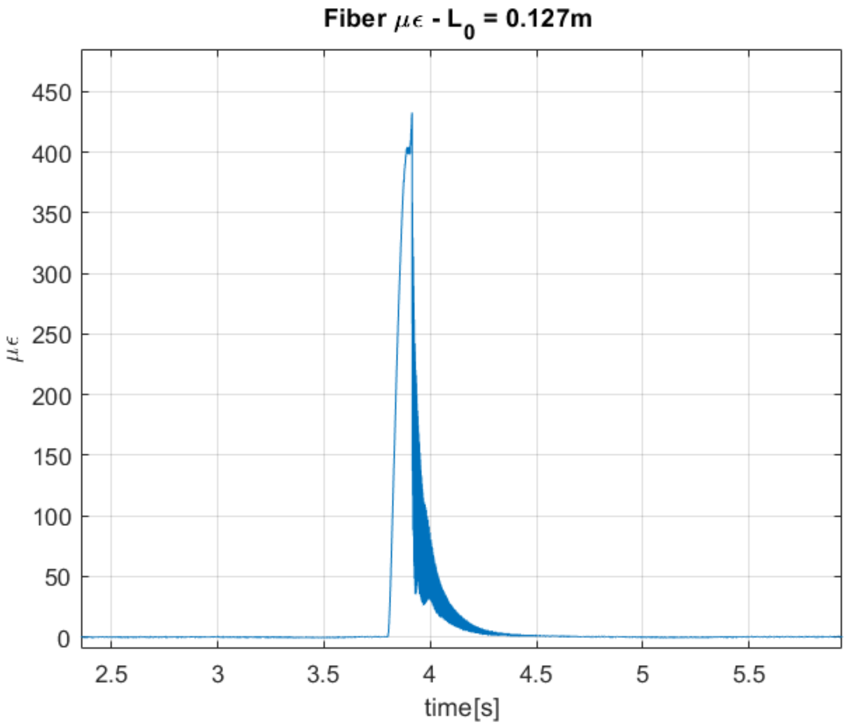

Figure 7.8: Fiber's own frequency experimentally estimation, effective length 0.127 m

At ≈ 3.7 seconds the fiber is pinched and continue its vibration until ≈ 4.3 seconds. The experimental natural frequency estimation produce a value of 1250 Hz.
Inserting T correspondent to 1000 $\mu\epsilon$, L and f values in equation 7.4, the ρ value obtained is:

$$\rho \approx 3.8 \cdot 10^{-6} \; \frac{kg}{m}$$

If the ρ value computed is used on fibers with different effective lengths and the frequencies estimatad experimentally and theoretically are comparable, it assumes that the ρ value's estimation is correct.

7.2.3 Results & Conclusions

This subsection's purpose is the comparison between the natural frequencies estimated experimentally and theoretically, in order to validate the behaviour of the fiber as a vibrating string. Moreover it will be possible better explain what said in subsections 6.1.3 and 6.2.1.
It is clear, looking at the equation 7.2, that the effective length of the fiber and the pretension on it affect the natural frequency calculation. Tests with different pretensions and effective lengths have been made.

Effective length L_0 = 0.1 m
Tests at a pretension of 500 $\mu\epsilon$ and 1000 $\mu\epsilon$ have been made.

ϵ	**T** [N]	**Theoretical Frequency** [Hz]	**Experimental Frequency** [Hz]
$500 \cdot 10^{-6}$	0.1887	1107	1250
$1000 \cdot 10^{-6}$	0.3774	1565	1562

Table 7.2: Natural frequency estimations, $L_0 = 0.1$ m

Effective length L_0 = 0.45 m
A second fiber with effective length of $L_0 = 0.45$ m has been used. According to the standing waves theory equation, a substantial decrease of the natural frequency is expected. Tests at 500 $\mu\epsilon$ and 1000 $\mu\epsilon$ have been conducted.

ϵ	**T** [N]	**Theoretical Frequency** [Hz]	**Experimental Frequency** [Hz]
$500 \cdot 10^{-6}$	0.1887	246	297
$1000 \cdot 10^{-6}$	0.3774	348	357

Table 7.3: Natural frequency estimations, $L_0 = 0.45$ m

The results of the two fibers, listed in table 7.2 and 7.3, show that the natural frequencies are comparable.
The fiber is actually acting as a vibrating string, so its behaviour is explanable according to the standing waves theory equations.
In particular, it is visible how the fiber's own frequency increase as the tension is increased and how it decrease if the effective length is increased.

What said, can explain the amplification values found during the high frequency tests, figure 6.10, and the pretension effects of figures 6.9 and 6.12. The fiber used in test of figure 6.10 has a natural frequency of $\approx$ 1562 Hz, it is possible that its own frequency influence the test as early as 150-200 Hz, which determines in this way a large front of amplification.
This has also been confirmed varying the fiber's tension: let's consider figure 6.12 tests. It is expected that the more the natural frequency is high, the less the test's values will result affected. This means that at the same frequency, for example 200 Hz, lower values of amplification are expected with higher values of pretension, figure 6.12 shows exactly what has just been said.
In this way it has been explaned the influence of the pretension on the high frequency tests, what about low frequency tests of figure 6.9? In this case, the natural frequency of the fiber (1562 Hz) does not affects the values because the frequencies used are too far from the fundamental one, so, under these conditions, the fiber's pretension on low frequencies tests has no relevance.
It is clear now that "low" and "high", as "near" and "far", are terms relative to the fiber's fundamental frequency.
Considering these results, it can be assumed that the natural frequency is the cause of the amplification values found during the high frequency tests.

Chapter 8

Conclusions & Future Works

In this chapter are collected all the ideas, tips and advices which can contribute to improve and re-design the test bench setup in order to obtain correct measures.
In the light of the above, it is clear that the whole measurement system has some limitations, first of all the test bench developed in this thesis suffer the fiber's natural frequency influence due to its nature of vibrating string, moreover the code can be improved or rewrited following another point of view. All of these problems have born from the inexperience and by the non complete knowledge of the hardware used.
It has been discovered that some operations conducted by the MATLAB code are negligible, the MATLAB code has been written trying to replicate the working logic of the PIMikroMove software, which works "by points", and it needs a lot of informations that the user must manually insert. Moreover in some limit cases, due to the discrete nature of the interrogator, it starts to generate "random" numbers when the signal's amplitude are near the sensivity of the interrogator. These are only few examples of what is improvable.
To resolve these problems, the code can be rewrited exploiting the sign of the derivative of the signal, freeing the user from inserting the values, and applying a well made filter, in order to dampen the noise produced by the interrogator, which affects heavily the measure at small amplitude. In addition to this the whole process may be fully automatized, in this way the user work will be limitated to execute and the tests, once all the files are saved the code may take them, process and display the computed values.
Considering the test bench setup, the fiber should be damped, the easiest

way is adding a mass. This solution is not applicable, first of all it is not really practical, secondly every mass added will influence the measure since that the mass of the suspended fiber is really small. At this point a redisgn of the test bench is then necessary.
In figure 8.1 is shown an idea of the new setup. In this concept are necessary two blocks of micropositioners, each block is composed by two micropositioners placed one over each other with the motion direction one perpendicular to the other. On the two blocks is glued the fiber and them are placed one per side respect to the piezoelectric actuator.

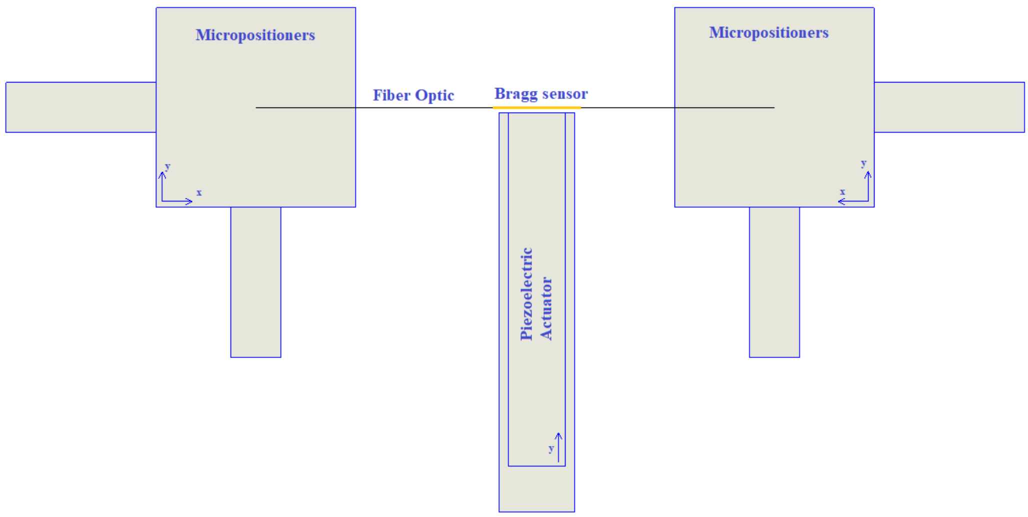

Figure 8.1: New test bench setup idea

In this way it will be possible to pretensionate the fiber with the couple of micropositioners which moves horizontally, and it will be possible approach the fiber to the actuator with the other couple of micropositioners. The idea is to approach fiber and actuator until they touch theirself, and then conduce the tests as done during this thesis. In this way the problem of the damping will be avoided and a real sensor of vibration will be made.

Appendix

The value of the linear mass ρ computed in section 7.2.2, which has provided the tensions in section 7.2.3, has been calculated by the equation 7.4, with the tension value calculated with the Young modulus found in literature [20]. It is possible to calculate the fiber linear mass density ρ in another way, let's see how.
Reminding the equation 7.3, the tension of the fiber is proportional to the product $E_G \cdot A$, which can be estimated by making proportions in base of the material's quantity in the fiber's layers.
In this thesis, polymide fibers have been used, these fibers have core and cladding made by silica and coating made by polymide. Knowing the diameter, and so the area of each fiber layer, and the Young modulus of the single material, it is possible to obtain the products $E_G \cdot A$.
Table 8.1 reminds the fiber's layer characteristics and show their young modulus.

Layer	$\phi[\mu m]$	**Material**	**E [GPa]**
Core	9.6	Silica	72
Cladding	125	Silica	72
Coating	155	Polymide	2.5

Table 8.1: Fiber's layer features and materials' Young modulus

Considering the fiber's whole diameter, it is essentially made by silica until 125 μm, and made by polymide from 125 to 155 μm. So the mean $E_G \cdot A$ product is:

$$E_{G_{silica}} \cdot A_{silica} + E_{Gpolymide} \cdot A_{polymide} =$$

$$72 \cdot 10^9 \cdot \frac{\pi \cdot 0.000125^2}{4} + 2.5 \cdot 10^9 \cdot \frac{\pi \cdot 0.000030^2}{4} = 885.3\ GPa \cdot m^2$$

The same product, calculated with the value of the Young modulus found in literature and the fiber section total area, was:

$$20 \cdot 10^9 \cdot \frac{\pi \cdot 0.000155^2}{4} = 377.4\ GPa \cdot m^2$$

The values difference is considerable, it will affect significatively the ρ value calculation. Using the same data of natural frequency, 1250 Hz, effective length, 0.127 m, and pretension, 1000 $\mu\epsilon$, used in ρ **value calculation** paragraph, the new value of the fiber density linear mass is

$$\rho \approx 9 \cdot 10^{-6}\ kg/m$$

The ρ will also affect the tension values computed and listed in table 7.2 and 7.3 but, considering that the term $\sqrt{\frac{T}{\rho}}$ of the 7.2.3 equation is constant, the frequency values computed will not be affected, making the standing wave theory still valid.

Bibliography

[1] Tosi Daniele, Perrone Guido, *Fiber optic sensor for biomedical application*, Artech house, 2018, cap 1, cap 5.

[2] D. K. Bhattacharya, Poonam Tandon, *Engineering physics*, Oxford University Press, 2015, cap 5.

[3] Schubert, E. Fred, *Light-Emitting Diodes (2nd edition)*, Cambridge University Press, 2010, cap 22.

[4] Xiao Xinran, Loos Alfred, Liu Dashin, *Proceedings of the American Society for Composites 2015-Thirtieth Technical Conference*, DEStech Publication, 2015, pag 2343.

[5] Stephen W. James and Ralph P. Tatam, *Optical fibre long - period grating sensors characteristics and application*, Institute of Physics Publishing, 2002, page 1.

[6] Turan Erdogan, *Fiber Grating Spectra*, Journal of lightwave technology - vol. 15, 1997.

[7] Xiaojing Zhang, Zhanjun Wu, Boming Zhang, *Strain dependence of fiber Bragg grating sensors*, Optical engineering,2006.

[8] Smartscan, *Smartscan datasheet.*

[9] B. Suresh; M. Sumedha; T. Visalakshi; K. Naveet, *Piezoelectric Materials - Applications in SHM, Energy Harvesting and Bio-Mechanics*, 2017, John Wiley and Sons, introduction.

[10] T. Markku; M.Teruaki; A. Veli-Matti; F. Sami; P. Krckel *Handbook of Silicon Based MEMS Materials and Technologies (2nd Edition)* Elsevier,2015, cap.1

[11] PI, *PI LISA Linear Actuator and Stage datasheet.*

[12] PI, *PI E-500/E-501 datasheet.*

[13] PI, *PI E-509 datasheet*

[14] PI, *PI E-802 servo-controller submodule datasheet*

[15] Giancarlo Candiano, *Fiber Bragg Grating Sensors for Mechanical and Thermal Prognostics and Diagnostics for Aerospace Application*, Politecnico di Torino,2018.

[16] SmartSoft, *SmartSoft v4.1 user manual*

[17] PI,*PIMikroMove software manual*

[18] Pal, Bishnu P. ; *Guided Wave Optical Components and Devices - Basics, Technology, and Applications* , Elsevie, 2006, Cap.17

[19] ANALOG DEVICES, *ADXL 345 datasheet*

[20] P. Antunes, F. Domingues, M. Granada P.Andre; *Mechanical Properties of Optical Fibers*; Universidade de Aveiro